EXPERIMENTS ON YIELDING OF TENSION SPECIMENS WITH NOTCHES AND HOLES.

By

EŞREF DOĞAN

ACKNOWLEDGEMENT

The author wishes to express his sincere gratitude to Dr. Walid Hasan Rimawi for the invaluable time he has devoted in directing the thesis and reviewing the manuscripts.

A special debt of gratitude is owed to Dr. Kâşif Onaran who, through his advise and help over measuring techniques contributed much.

The author also wishes to express his appreciation to his school-mates, in particular to

Hüsamettin Alper
Lütfi Sari
Yavuz Çizmeci
Hamdi Ataoğlu
Hüseyin Iğdirli
Halim Aydin

for their generous help in the preparation and testing of samples and to Sedat Özmen for his kind help in taking and developing various pictures included in the thesis.

Special thanks are due to Tamer Tunca for the invaluable time he had devoted to the drawings presented in the paper.

Finally, the untiring efforts of Patricia Gülsen Karşit and Nusret Taşlica need to be mentioned with author's gratitude.

E. D.

Robert College, Istanbul

TABLE OF CONTENTS

CHAPTER I

INTRODUCTION

1.1 (a) Definition of Plasticity

Theory of plasticity is the name given to the mathematical study of stress and strain in plastically deformed solids, especially metals. Its starting point is certain experimental observations of the macroscopic behavior of a plastic solid in uniform states of combined stress. The task of the theory, as stated by Hill (1)* is twofold; first, to construct explicit relations between stress and strain agreeing with the observations as closely and universally as need be; and second, to develop mathematical techniques for non-uniform distribution of stress and strain in bodies permanently distorted in any way.

The theory of plasticity is especially concerned with the technological forming processes, such as the rolling of strip, extrusion of rods and tubes, drawing of wire, and deep-drawing of sheets which involve very large plastic strains (2) and deformations. In this case elastic strains may be ignored. Intense plastic strains may be also produced locally in many mechanical tests such as indentations by a conical die. The bending of a notched bar, or the extension of a tensile specimen past the necking point. However, in determining the yield load large strains are not involved. In order to be able to account for the significance of those phenomena a knowledge of state of stress and strain in the plastic zone is required. Plastic strains of eleastic order may be of prime importance to the structural and machine designer. With the great premium currently placed on the saving of weight in aircraft, missile, and space applications, the designer can no longer use large factors of safety and "beef up" his design. He must design for the maximum load to weight

---

(*) Number in the brackets refer to the References at the end of the thesis.

ratio, and this inevitably means designing into the plastic range (2). Elasto-plastic situation is involved in structural applications when it is necessary to predict the critical loading which just causes a structural member to start yielding plastically.

1.1 (b) Historical Background

Coulomb (1) had proposed the criterion for yielding of soils in 1773. However, the scientific study of the plasticity of metals had begun by Tresca (1864) (1) when he published a preliminary account of experiments on punching and extrusion. He stated that metal yielded when the maximum shear stress attained a critical value. Poncelet (1840) and Rankine (1853) applied the Coulomb's yield criteria to the problems of earth-pressure on retaining walls. Saint-Venant (1870) used Tresca's yield condition to determine stresses in a partly plastic cylinder subjected to a combined bending and torsion. In 1871 Levy, adopting Saint-Venant's conception of an ideal plastic material, proposed three-dimensional relations between stress and rate of plastic strain. Later, Guest, in England, investigated the yielding of hollow tubes under combined tension and internal pressure. Haar, and Von Karman contributed much to the field. In 1913 von Mises on the basis of purely mathematical consideration presented his famous yield criteria which was interpreted by Hencky some years afterwards as implying that yielding occured when the elastic shear-strain energy reached a critical value.

Germans were active between two wars. 1920-21 Prandtl showed that two dimensional plastic problem is hyperbolic (1). Hencky supplied the general theory underlying Prandlt's work; he also discovered the simple geometric relations of the slip-lines in a state of plane strains. In 1923 Nadai investigated plastic zones in a twisted bar. In 1925 Von Karman analyzed, by an elementary method state of stress in rolling. Siebel and Sachs put forward similar theories for wire-drawing.

In 1926 Lode showed that Levy-Mises stress-strain relations were valid to a first approximation. Taylor's and Quinney's experiments (1931) confirmed certain divergences that Lode's experimental results have indicated. Theory was generalized in two directions: Reuss (1930) made allowance for elastic component of strain, and Schmidt (1932) and Odquist (1933) showed how work-hardening could be brought within the frame work of Levy-Mises equations. Hohenemer (1931-2) proved the works of Reuss, whereas, investigations of Schmidt confirmed the hypothesis of Odquist and himself. Therefore, a theory had been constructed then on.

Later on a rival theory proposed by Hencky came into use especially by Nadai; and afterwards by the Russian School. Although the plastic strains were small, experiments showed that one to one relation did not exist.

After the Second World War, England and U.S.A. had earned extensive researches which is still going on. Brown University in U.S.A. has been a leading center of Plasticity engaged in theoretical studies. Lehigh University became a research center of plastic design methods (3). There, problems of instability have also been studied. Baker and his associates have studied the behavior of frame members which failed by building and position reached by 1956 was described in The Steel Skeletons. Concept of plastic hignes and stability of frames was studied by Merchant, Wood and Horne. Baker was the first to realize that the simple plastic theory might well prove to be the key solution and a rational method for design of complex frames. Calculating Baker formal statements and proofs of plastic collapse load were published by Greenberg and Poager, and by Hodge although an earlier paper by Gvozdev, in which these principles were established had appeared in 1938.

Hill in his famous book "The Mathematical Theory of Plasticity" and numerous papers contributed much to the theoretical field of plasticity.

Johansen (4) in Sweeden had developed the yield line theory basically for plastic plates. It seems that researches carried under the sponsorship of NATO (5) will add a lot of new things to the chain of scientific studies in plasticity.

1.2 Inelastic Behaviour

The main characteristic of the mechanical behaviour of an elastic material is adequately expressed by Hooke's famous statement "ut tensio sic vis" (6). However, no simple description of the mechanical behaviour of the plastic material is possible, and a mathematical theory attempting to take account of all mechanical phenomena observed in the plastic range would not be practical.

The generalization of Hooke's Law to three dimensions for an isotropic material, using the tensor notation and, including thermal strains becomes*

$$\varepsilon_{ij} = \frac{1}{2G}\,\sigma_{ij} - \delta_{ij}\left(\frac{\mu}{E} I - \alpha T\right) \qquad (1.1)$$

where E is the Young's Modulus, μ Poisson's ratio, α the coefficient of linear thermal expansion, T the temperature above some arbitrary reference temperature, G, the shear modulus of elasticity and

$$I = \sigma_x + \sigma_y + \sigma_z$$

ε_{ij}, σ_{ij}, and δ_{ij}, are the strain tensor, the stress tensor and the kronecker delta respectively.

For sufficiently small values of stress and strain, test specimen reassume their original shape upon unloading. In other words, they behave elastically and Hooke's Law is applicable.

(*) In Equation (1.1), index notation is used in which an index i takes the values 1, 2, 3 (x,y,z). Repeated indices means Summation and comma means differentiation with respect to the space coordinates.

For values beyond the elastic limit, the specimen will not reassume its original shape upon unloading, but will show a permeanent deformation. In other words, it will behave inelastically. There is no more a one-to-one correspondence between the load and deformation as shown in Figure 1.

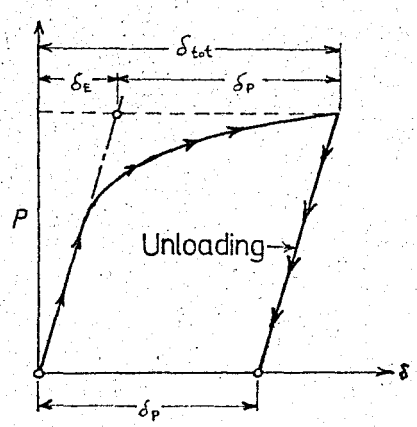

Figure 1
Effect of loading beyond the elastic range.

Permanent deflection or permanent set δ_p will be equal to the total deflection minus elastic deflection (7):

$$\delta_p = \delta_{tot.} - \delta_E$$

An interesting phenomenon observed in the test of many materials is that reloading after unloading will cause only elastic deflections almost up to the load which had previously been applied then causing a rise in the proportional limit. Fig.2.

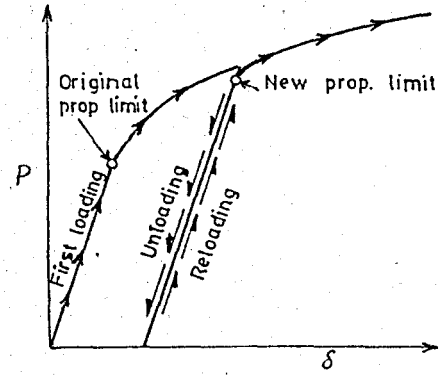

Figure 2
Effects of reloading.

Many materials will show an abrupt change, flattening of the force deflection curve when a certain load is reached. Then a large ammount of deflection will occur with little increase in loading. It is often convenient to show such behaviour by idealized stress-strain diagrams consisting of two straight lines. Figure 3 (a).

The behaviour in which the deflection increases without any increase in load is called ideally plastic. In some cases elastic strains are entirely neglected as shown in Figure 3 (b) or both elastic and plastic behaviour may be included. The term elastic-perfectly plastic is often employed to define the idealization shown in Figure 3 (a).

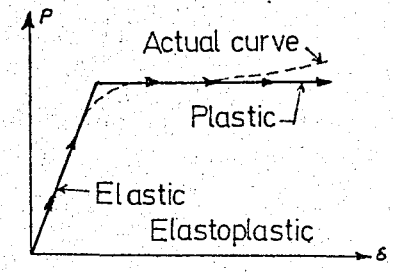

(a)

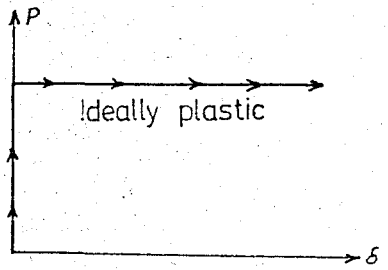

(b)

Figure 3

Idealized force-deflection curves.

1.3 The Criterion of Yielding

(a) General Considerations

A law defining the limit of elasticity under any possible combination of stresses is known as a criterion of yielding (1). Yield stress is the one which corresponds to some arbitrary permanent strain set after the elastic limit (7).

Factors which have an influence on the magnitude of the forces under which a material will yield plastically may be stated as (8) :

1) The structure of material as dependent on the constitution of the substance especially of alloys.

2) The absolute size of the crystal grains constituting a polycrystalline material.

3) The imperfections and disturbances in the crystal lattice.

4) Temperature.

5) Time.

Assuming material to be isotropic, plastic yielding then depends on the magnitude of the three principal stresses applied and not on their directions. Any yield criteria is expressible in the form (1)

$$f\left(I_1, I_2, I_3\right) = 0 \qquad (1.2)$$

where I_1, I_2, I_3 are the three stress invariants. In terms of principal stresses,

$$I_1 = \left(\sigma_1 + \sigma_2 + \sigma_3\right), \quad I_2 = -\left(\sigma_1\sigma_2 + \sigma_2\sigma_3 + \sigma_3\sigma_1\right), \quad I_3 = \sigma_1\sigma_2\sigma_3 \qquad (1.3)$$

Any function of the invariants can be expressed in terms of the principal stresses, it is not true that any function of the principal stresses represents a possible yield criteria. The function f is the characteristic of the state of the metal before unloading, and therefore depends on the heat and mechanical treatment of the metal.

The experimental fact reveals that yielding of a metal, to a first approximation is unaffected by a moderate hydrostatic pressure or tension either applied alone or superposed on some

state of combined stress. If this is strictly true for ideal plastic body, it follows that yielding depends on the principal components ($\sigma_1', \sigma_2', \sigma_3'$) of the deviatoric or reduced, stress tensor (1)

$$\sigma_{ij}' = \sigma_{ij} - \sigma \delta_{ij} \tag{1.4}$$

where $\sigma = \frac{1}{3}\sigma_{ij}$ is the hydrostatic component of the stress. The principal components are not independent, since $\sigma_1' + \sigma_2' + \sigma_3'$ is identically zero. Therefore, the yield criterion reduces to the form

$$f(I_2', I_3') = 0 \tag{1.5}$$

where

$$I_2' = (\sigma_1'\sigma_2' + \sigma_2'\sigma_3' + \sigma_3'\sigma_1')$$

$$I_3' = \sigma_1'\sigma_2'\sigma_3' \tag{1.6}$$

Also, it is assumed that ideal plastic body does not show a Bauschinger effect, therefore it has same yield stress in tension and compression. And since, I_3' changes sign when the stresses are reversed, it follows that f must be an even function of I_3' (1).

(b) Examples of Yield Criteria

The idea of yield criterion goes as far back as Coulomb in 1773 when he had attempted to explain failure of soils. Many of the criteria developed then on were suggested as criteria for failure of the brittle metals. Later on, they were adopted as yield criteria for ductile materials. Because of their historic values some of them will be briefly mentioned here, and the ones that are practised today will be explained in detail.

1) Maximum Stress or Rankine Theory

This theory assumes that yielding occurs when one of the principal stresses becomes equal to the yield stress in simple tension σ_o , or the yield stress in compression $\sigma_{o,c}$. This

theory shows very poor agreement with experiment and is rarely used. According to this theory, then all material should yield plastically when subjected to sufficiently high hydrostatic pressure (8). We have already stated that this was not true.

2) Maximum Strain Theory or Saint-Venant Theory

This theory assumes that yielding will occur when the maximum value of the principal strain equals the value of the yield strain in simple tension (or compression). This does not agree well with most experiment (2). For, undersufficiently high hydrostatic pressure, the maximum limiting strain must certainly be reached, and therefore, according to this theory the material should fail (8). This is not the case since most metals can withstand any arbitrary amount of hydrostatic pressure without failure or without starting to yield plastically.

3) Maximum Shear Theory or Tresca's Criterion

Tresca (1864) assumed that yielding will occur when the maximum shear stress reaches the value of the maximum shear stress occuring under simple tension

$$\tau_{max} = \pm \frac{1}{2}\left(\sigma_1 - \sigma_3\right) \qquad (1.7)$$

where σ_1 = maximum and σ_3 = minimum principal stresses. For simple tension $\sigma_2 = \sigma_3 = 0$

$$\tau_{max} = \frac{1}{2}\sigma_0 \qquad \text{(Maximum shear stress at yielding).}$$

A plot in $\sigma_1\sigma_2$ plane for this yield criteria is shown in Figure 4. It is to be noted that one limitation of this theory is the requirement that the yield stress in tension and compression be equal (2). Though widely used, it suffers one major difficulty - it is necessary to know in advance which are the maximum and minimum principal stresses.

For a case of pure shear $\sigma_1 = -\sigma_2 = k$, $\sigma_3 = 0$

$$k = \frac{\sigma_0}{2} \qquad (1.8)$$

where k is the yield stress in simple shear.

4) Mises Criteria or Distortion Energy Theory

Mises assumed that yielding occured when I_2' reached a critical value in alternative forms yielding would occur when I_2' reached the value of I_2' at yielding in simple tension, or

$$I_2' = \frac{1}{3}\sigma_o^2 \qquad (1.9)$$

which when written in terms of total stress components takes the form

$$(\sigma_x - \sigma_y)^2 + (\sigma_y - \sigma_z)^2 + (\sigma_z - \sigma_x)^2 + 6(\tau_{xy}^2 + \tau_{zx}^2 + \tau_{yx}^2) = 2\sigma_o^2 \qquad (1.10)$$

A physical interpretation given by Hencky was that equations 1.9 and 1.10 implied that yielding begins when the recoverable elastic energy of distortion reaches critical value. According to Hill (1) this may not have a general significance. When we have a biaxial case Mises yield criterion takes the form

$$\sigma_1^2 - \sigma_1\sigma_2 + \sigma_2^2 = \sigma_o^2 \qquad (1.11)$$

This is the equation of an ellipse, called von Mises Ellipse as shown in Figure 5.

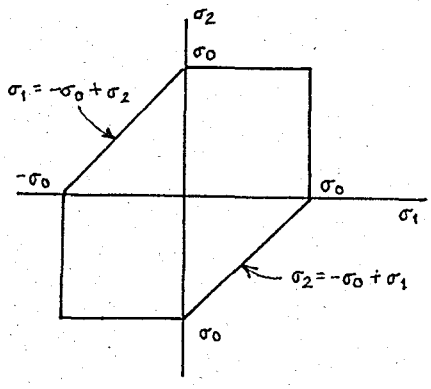

Figure 4
Maximum Shear Stress Theory

For a case of pure shear, $\sigma_1 = -\sigma_2 = k$, $\sigma_3 = 0$ and equation 1.11 yields

$$k = \frac{\sigma_o}{\sqrt{3}} \qquad (1.12)$$

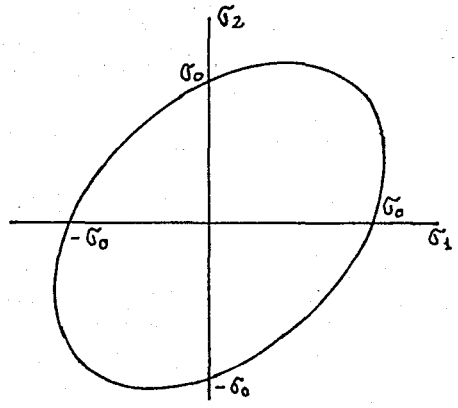

Figure 5
Distortion Energy Theory

That is yield stress in pure shear is $1/\sqrt{3}$ times the yield stress in simple tension. Therefore, the Mises criteria predicts a pure shear yield stress 15 % higher than predicted by Tresca's yield condition.

For most metals von Mises criterion fits the data more closely than Tresca's. However, because of its simple form Tresca criterion is also used in some applications.

1.4 Stress-Strain Relations

(a) Elastic Behaviour - Generalized Hookes' Law

The state of a stress in continuous media is completely determined by the stress tensor σ_{ij} , and the state of deformation by the strain tensor ε_{ij} . When an elastic medium is maintained at a fixed temperature there is one-to-one analytic relation

$$\sigma_{ij} = F_{ij}\left(\varepsilon_{11}, \varepsilon_{22}, \varepsilon_{33}, \ldots\ldots\ldots \varepsilon_{12}\right) \qquad (1.13)$$

between σ_{ij} and ε_{ij}. If Fij is expanded in the power series in ε_{ij}, and only linear terms retained, the following is obtained

$$\sigma_{ij} = C_{ijkl}\,\varepsilon_{ij} \qquad (i,j,k,l = 1,2,3) \qquad (1.14)$$

where Cijkl are the material tensor, and symmetric with respect to first and last two indices.

When an isotropic, homogeneous media is considered, the number of essential elastic constants reduces to 2 (9). Thus, the generalized Hooke's Law for a homogeneous isotropic body can be written in the form

$$\sigma_{ij} = \lambda \delta_{ij} J + 2\mu_o \varepsilon_{ij} \tag{1.15}$$

λ and μ_o are the Lame constants, and J is equal to ε_{ii}. Substituting the following relations (10)

$E = \frac{\mu_o(3\lambda + 2\mu_o)}{\lambda + \mu_o}$ (Young's Modulus), $\nu = \frac{\lambda}{2(\lambda+\mu_o)}$ (Poisson's Ratio)

in equation 1.15 leads to the well known Generalized Hooke's Law.

$$\begin{aligned}
\varepsilon_{xx} &= \frac{1}{E}\left[\sigma_{xx} - \nu\left(\sigma_{yy} + \sigma_{zz}\right)\right] \\
\varepsilon_{yy} &= \frac{1}{E}\left[\sigma_{yy} - \nu\left(\sigma_{zz} + \sigma_{xx}\right)\right] \\
\varepsilon_{zz} &= \frac{1}{E}\left[\sigma_{zz} - \nu\left(\sigma_{xx} + \sigma_{yy}\right)\right] \\
\varepsilon_{xy} &= \frac{1+\nu}{E}\,\tau_{xy} \\
\varepsilon_{yz} &= \frac{1+\nu}{E}\,\tau_{yz} \\
\varepsilon_{zx} &= \frac{1+\nu}{E}\,\tau_{zx}
\end{aligned} \tag{1.16}$$

In an elastic solid the following relations should hold in addition to Generalized Hooke's Law, Equation 1.15.

1) Equilibrium

$$\sigma_{ij,i} = -F_j \tag{1.17}$$

where Fj are the body forces.

2) Boundry conditions.

$$\sigma_{ij}\, n_j = T_i \tag{1.18}$$

where Ti is the traction, and nj is the unit normal perpendicular to the surface considered (9).

3) Compatibility

$$\varepsilon_{ij,kl} + \varepsilon_{kl,ij} - \varepsilon_{ik,jl} - \varepsilon_{jl,ik} = 0 \qquad (1.19)$$

of these 81 eqations only six are independent. Equations 1.19 ensure the continuity of displacements and therefore are known as equations of compatibility (9).

4) Strain - displacement relations

$$\frac{1}{2}\left(u_{i,j} + u_{j,i}\right) = \varepsilon_{ij} \qquad (1.20)$$

(b) Plastic Behaviour

In the plastic range, there is no one-to-one correspondence anymore, between the stress and strain. Yield criteria is not enough to characterize the mechanical behaviour of a plastic material. It must be supplemented by the stress-strain relations for the plastic range.

The general equations for determining the plastic stress-strain relations for any yield criteria is presented on a unified approach due to Drucker (2).

Work hardening implies that when an external agency applies a set of an additional stresses on a given state of stress and then slowly removes them, material will remain in equilibrium, and:

1. Positive work is done by the external agencies during the application of the set of stresses.
2. The net work performed by it over the cycle of application and removal is zero or positive.

Under stress increments $d\sigma_{ij}$, we have $d\varepsilon_{ij}$, then for work hardening from implication 1

$$d\sigma_{ij}\, d\varepsilon_{ij} > 0 \qquad (1.21)$$

and from implication 2.

$$d\sigma_{ij}\left(d\varepsilon_{ij} - d\varepsilon^{e}_{ij}\right) \geq 0$$

$$d\sigma_{ij}\left(d\varepsilon^{e}_{ij} + d\varepsilon^{p}_{ij}\right) > 0 \qquad (1.22)$$

or

$$d\sigma_{ij}\, d\varepsilon_{ij} > 0$$

Equations (1.22) represent mathematical definition of "workhardening. Second equation is sometimes referred as "the uniqueness condition."

To obtain the general stress-strain relations, we use the above definitions plus two basic assumptions:

1. A loading function exists. At each stage of the plastic deformation there exists a function $f(\sigma_{ij})$ that further plastic deformation takes place for $f(\sigma_{ij}) > K$. Both f and K may depend on the existing state of stress and on the strain history.

2. The relation between the infinitesimal of stress and plastic stain is linear, i.e.,

$$d\varepsilon_{ij}^{p} = C_{ijkl}\, d\sigma_{kl} \qquad (1.23)$$

This is purely an assumption. C_{ijkl} may be a function of stress strain and history of loading, but above equations imply that they are independent of σ_{kl}.

From the first one

$$df(\sigma_{ij}) > 0 \qquad (1.24)$$

or

$$\frac{\partial f}{\partial \sigma_{ij}} d\sigma_{ij} > 0$$

so that plastic deformations takes place. Second assumption asserts that principle of superposition may be applied. (2)

From eqs. (1.21) to (1.24) a stress strain increment relation may be written in the form

$$d\varepsilon_{ij}^{p} = G \frac{\partial f}{\partial \sigma_{ij}} df \qquad (1.25)$$

where G is a scalar which may depend on stress, strain and history.

To calculate the plastic strains at a final load condition it is theoretically necessary, in general, to integrate the infinitesimal plastic strain increments over the actual path of loading.

For a perfectly plastic material eq. (1.25) takes the form

$$d\varepsilon_{ij} = d\lambda \frac{\partial f}{\partial \sigma_{ij}} \qquad (1.26)$$

where $d\lambda$ is a scalar.

Drucker's Postulate leads to the prove of convexity of the yield surface and the stress strain increment relations which are the building blocks of theory of plasticity (5),(11).

1.5 Limit Analysis

a) General consideration

The results which are to be presented here are due to Drucker, Greenberg and Prager taken from the "Limit Analysis in Plane Strain" section of "Theory of Perfectly Plastic Solids", by Prager and Hodge*.

A generic cross-section R (see Fig. 6) is considered which has a boundry B, H is assumed that boundry B consist of

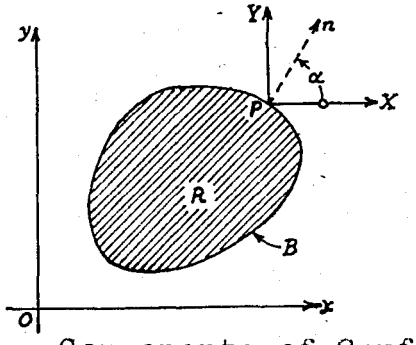

Figure 6 - Components of Surface Traction

finite number of arcs which will fall into one of the following categories:

1) Arcs along which the vector of the surface traction is prescribed, or

2) Arcs along which the displacement vector must vanish.

An application of proportional, continual loading is

---

* Reference (6)

assumed. It is supposed that given surface tractions are sufficiently small so that we won't exceed range of contained plastic flow. When a state of impending plastic flow is reached, we shall have an increase in plastic strain under constant load. The ratio of a generic surface traction at the instant of impending plastic flow to the given value of this surface traction will be called "Factor of safety". It is important to note that up to the point of impending plastic flow equilibrium and boundry conditions of undeformed rather that deformed body are satisfied.

There are two theorems guiding the lower and upper bounds for this safety factor. At this stage it will be usefull to define some terms which have originally been developed by Greenberg and Prager. (12).

b) Statically Admissible Stress Field- Lower Bound.

A continuous or discontinuous stress field satisfying.

1) Equations of equilibrium

$$\frac{\partial \sigma_x}{\partial x} + \frac{\partial \tau_{xy}}{\partial y} = 0$$
$$\frac{\partial \tau_{xy}}{\partial x} + \frac{\partial \sigma_y}{\partial y} = 0 \qquad (1.27)$$

throughout R, or throughout each finite subregions into which R is divided.

2) The boundry conditions along each boundry of the arc where surface traction is prescribed, and

3) The yield inequality

$$(\sigma_x - \sigma_y)^2 + 4\tau_{xy}^2 - 4k^2 \leq 0 \qquad (1.28)$$

is called statically admissible stress field. An example for a notched tension specimen is shown in Figure 7..

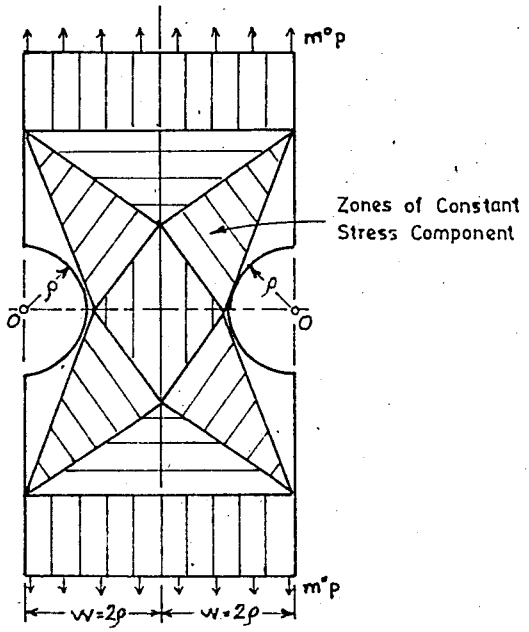

Figure 7 - Statically Admissible Stress Field

A number m° is called statically admissible multiplier if there exists a statically admissible stress field, such that nowhere yield is exceeded, for surface tractions $m^\circ X$, and $m^\circ Y$ (2). The Lower Bound Theorem states that the safety factor is the largest statically admissible multiplier. It is the case when the equilibrium distribution of stress balances the externally applied load and is anywhere below yield or at best at yield.

c) Kinematically Admissible Velocity Field Upper Bound

A velocity field, continuous or discontinuous satisfying

1) Conditions of incompressibility

$$\frac{\partial v_x}{\partial x} + \frac{\partial v_y}{\partial y} = 0 \qquad (1.29)$$

2) The condition that velocity components v_x, v_y vanish along each finitie arc of B

3) And the condition that total external work rate is positive.

$$\int_B (X v_x + Y v_y)\, dS > 0 \qquad (1.30)$$

The multiplier m^* associated with the kinematically admissible velocity field is defined as the ratio of internal to external energy dissipations:

$$m^* = k \frac{\sum \int \dot{T} dA + \sum \int_{L_{hk}} |V_T^{(k)} - V_T^{(h)}| dL_{hk}}{\int_S (X v_x + Y v_y) dS} \qquad (1.31)$$

where

$$\dot{T} = \left[\left(\frac{\partial v_x}{\partial x} - \frac{\partial v_y}{\partial y} \right)^2 + \left(\frac{\partial v_x}{\partial y} + \frac{\partial v_y}{\partial x} \right)^2 \right]^{1/2}$$

is the maximum shear rate, L_{kh} is the line of discontinuity seperating regions R_h and R_k, $V_T^{(h)}$, the velocity component in the direction t_{hk} - the unit vector tangential to L_{hk}, on the side R_h of the line L_{hk}, and $V_T^{(k)}$ corresponding component on the side R_k. (See Figure 8.)

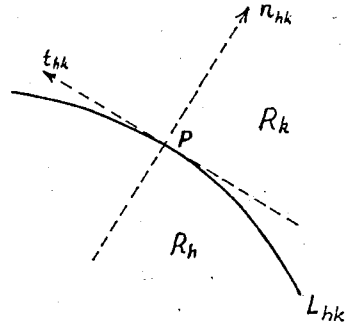

Figure 8 - Conditions at line of Discontinuity

k is the tangential stress transmitted across the boundry.

The Upper Bound Theorem states that the safety factor is the smallest kinematically admissible multiplier. Structure must collapse if there is any compatible pattern of plastic deformation for which rate of external work is equal to or exceeds the rate of internal energy dissipation.

Combining upper and lower bound theorems, the safety factor m is bound

$$m^o \leq m \leq m^* \qquad (1.32)$$

If $m^{o}p$ is the axial stress applied to the ends of the specimen in Figure 7, the result obtained is (6)

$$m^{o} = 1.26 \frac{k}{p} \qquad (1.33)$$

For Figure 9, the line AB is a line of discontinuity. Shaded

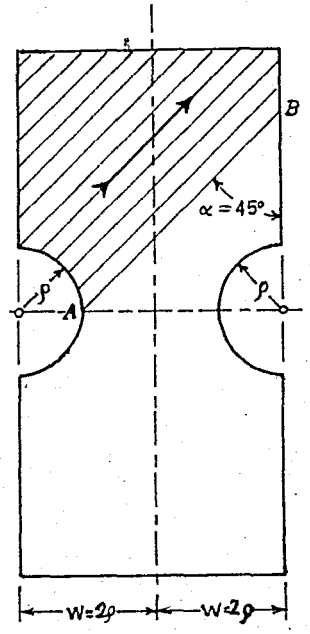

Figure 9 - Kinematically admissible Velocity Field

portion above this line moves as a rigid body with a unit velocity in the direction of arrow. Equation (1.31) gives:

$$m^{*} = \frac{k \cdot 3a\sqrt{2}}{1/2\ \sqrt{2}\ 4ap} = 1.5 \frac{k}{p} \qquad (1.34)$$

d) Discontinuity

The evaluation of the limit load under which unrestricted plastic flow sets in must frequently be based on discontinuous stress distributions.

Lines of discontinuity are the boundries of constant stress regions though defination could have included the stress fields of varying type too.

In Figure 10, L-L is a line of discontinuity, and α is the angle between x-axis and normal to this element. Regions are labelled as 1 and 2.

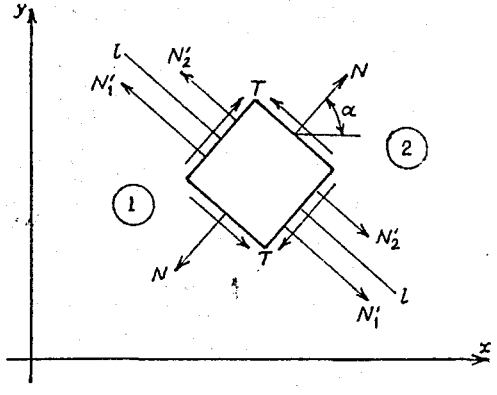

Figure 10 - Discontinuous Stresses in Problems of Plane strain

Equilibrium of the rectangular element shown, requires that exterior components of stress N and T are continuous across L-L. T is the tangential and N is the normal components of stress. However, the internal component, N' may be discontinuous without upsetting the equilibrium. Yield condition on both sides of the line of discontinuity must be satisfied.

Winger and Carrier (6) have shown that at least four fields of constant stress must meet a point where several lines of discontinuity meet. If conditions of equilibrium, and a yield condition are satisfied by the discontinous stress distribution, in connection with Figure (9), the only velocity field compatible with such a stress distribution corresponds to rigid body motion*

* Actually this statment is for a truncated wedge. However, since there are no stresses in region 5, when half of the discontinuous

Velocity component may be discontinuous also. Though velocity component normal to the line of discontinuity is continuous, the component tangnet to the line may vary in a discontinuous manner.

Line of discontinuity in the stress field must be considered as the limiting case of a thin elastic layer which provides a continuous transition from one plastic stress field to the other, where as line of discontinuity in velocity field must be regarded as the limiting case of a thin layer providing continuous transition from one velocity field to other. It can be proven that the line of discontinuity is either a shear line or an envelope of shear lines, i.e., a limiting line (6).

---

* (cont.) stress field is considered, it will behave like a truncated wedge.

CHAPTER II

EXPERIMENTAL WORK

2.1 INTRODUCTION

The foremost reason of any experimental stress analysis is to "avoid a failure" of the machine or structure. Because of the many difficulties involved in the use of physical properties, such as yield strength etc., safety factors or uncertainity factors have been devised to help bridge the gap between idealized test data and actual design practice.

Failure means any change in the physical shape, configurations or properties of member in which the change will seriously effect the satisfactory performance of that member within a machine or structure (13). Rupture, buckling, excessive deformation, extreme wear may be the chief causes of failure. Or some times when elastic strains or plastic strains of elastic order are of high importance failure will be assumed if the proportional limit is exceeded. *

The usual starting point of a rupture is at some stress raiser, or a point of high stress concentration within the member. What experimental stress analysis types to determine is the points of high stress concentration, and stresses exist there in order to avoid failure, or to locate the regions of low stresses in order to remove unnecessary weight without affecting the satisfactory performance of that member.

Notches and fillets are called "stress-raisers". Holes because they disturb the stress pattern cause stress concentration and premature failure of engineering materials. (13)

---

* Designs based on working stress

Recently studies on stress-raisers and cut-outs of various shapes gained importance in order that design of machine parts or structures based on minimum weight concept would safely be secured. Although a far developed theoretical background has been established for V-notched strips and holed strips, still experimental varification of theories prove to be useful and necessary.

In this paper, variation of the load causing the yield in a V-notched strip, as angle of notch changes from zero to 180, has been analyzed. In order to utilize the full strength of a notched member the angle or the angles for which the load that caused plastic flow was maximum, has been investigated.

In the second series of the test, as a cut-out in a structural member may be of any shape, effect of the various cut-outs on yield load has been searched for in order to be able to make a comparison among them and choose the best one for utilizing a certain purpose.

Eccentrically located circular holes, the third series of these experiments, are very common in structural engineering or machine design. An investigation of the load causing plastic deformation for a particular eccentricity (such as 2mm, 4mm and 6mm) has been carried to detect the safest load that a member can carry in accordance with the location of the hole. Since the possibility of punching or drilling holes eccentrically is very big, an overall safety factor for any reasonable eccentricity has been investigated.

2.2 Review of Experimental and Theoretical Work on Notches and Hole

A lot of empirical relations were found, and tables of stress-concentration factors have been prepared for engineering purposes. Many of those tables and empirical relations can be found in Civil Engineering, Mechanical Engineering or experimental stress analysis books (7, 14, 15, and 16).

However yielding of notched bars under tension, as a

problem of plasticity has started between 1945-50. In 1950 Southwell and Allen (1) have shown how the stress equations of a semi-circular notch could be solved by application of relaxtation method. Fried and Sachs worked on the constrainting effect of the notch. Hill treated the upper bound determination of V-notched and semi-circular notched tension specimen (17 and 18). Lee (19) has analysed the plastic flow in V-notched bars pulled in tension. Orowan (20) worked on notch brittleness and strength of metals.

Hodge (20), did some work on yield conditions in plane plastic stress, devoting much attention to notched bar in tension according to Mises yield criteria. Drucker (21), considering notched samples developed the criteria on obtaining plane stress or plane strain condition in plasticity. Later on, 1965, Drucker and Findley (21) carried on an experimental study on plane plastic straining of notched bars. Limit load for plane stress and plane strain values were determined. Recently, Mura, Rimawi and Lee (22) have worked on extended theorems of limit analysis for isotropic solids which were then generalized to include anisotropy. In connection with those extended theorems, a limit analysis of notched specimen under tension was presented by Rimawi, Lee and Mura (21).

2.3 Theory of Plane Problems - Plane Stress-Plane Strain

When we are dealing with elasticity, the most significant parameter is the ratio of the sheet thickness to radius of the discontinuity in the region of greatest stress concentration. For a perfectly plastic material of unlimited ductility this is of no importance (21). A material dimensions such as distance between notches, for the notched strips replaces above condition of elasticity.

For notches, Drucker (22) has found that a ratio of $t/b \geq 2.11$ is required for a plane strain condition where b is the net width and t is the thickness. If we have a slit, upper bound for P/bt, which is net average stress over the cross-section between notch roots would lead to the requirement that $t/b \geq 4.0$.

In the present work t/b is well below the limits set by Drucker making all the samples tested a case of plane stress. Such a distiction is necessary since the plane strain solution tc limiting stress on the net section of a notched speciment is (21)

$$\sigma_c = 2k\left[1+\left(\frac{\pi}{2}\right)-\alpha\right] \qquad (2.1)$$

compared to

$$\sigma_s = 2k \qquad (2.2)$$

where σ_s is the plane stress solution, k being the limiting shearing stress, α is the half angle of the notch. If $\alpha=\frac{\pi}{4}$, $\sigma_c/\sigma_s = 1.795$ which is of considerable magnitude. Drucker's analysis of limiting ratio of t/b was verified experimentally by Drucker and Findley (22).

a) Sliplines

In a state of plane strain the two orthogonal families of curves whose directions at every point coincide with those of maximum shear strain-rate are knwon as slip lines. They are the characterictics of the equations of plane strain which are hyperbolic (1). Two families of the slip-lines are labled as α and β shown in Fig. 11

If ϕ is the counter-clockwise angular rotation of α- line from x-axis, it can be shown that for the case of plane strain the shearing strain is k, and the normal stress is $p=-\frac{1}{2}(\sigma_1+\sigma_2)$

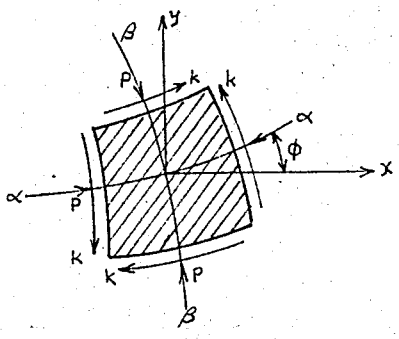

Figure 11
Stresses on a small curvilinear element bound by slip-line.

Then, the cartesian components of stresses become

$$\sigma_x = -p - k\,\mathrm{Sin}\,2\phi$$
$$\sigma_y = -p + k\,\mathrm{Sin}\,2\phi$$
$$\tau_{xy} = k\,\mathrm{Cos}\,2\phi \qquad (2.3)$$

These expressions are originally due to Lévy.

It can be proven that

$$p + 2k\phi = \text{Constant on an } \alpha\text{-Line}$$
$$p - 2k\phi = \text{Constant on a } \beta\text{-Line} \qquad (2.4)$$

These relations are completely equivalent to equilibrium equations. The constants may vary from one slip-line to the other.

Dealing with the velocity equations in a similar way, the following equations are obtained:

$$u_x = u\,\mathrm{Cos}\phi - v\,\mathrm{Sin}\,\phi$$
$$v_y = u\,\mathrm{Sin}\phi + v\,\mathrm{Cos}\,\phi \qquad (2.5)$$

where u and v are the velocity components referred to α-and β- lines (considered as a right-handed coordinate system).

It also can be shown that (1)

$$du - v\,d\phi = 0 \quad \text{along an } \alpha\text{-Line}$$
$$dv + u\,d\phi = \phi \quad \text{along a } \beta\text{-Line} \qquad (2.6)$$

These equations originally due to Geiringer, state that the rate of extension along any slip-line is zero.

Theory of slip lines was applied to notched bars in plane strain (19).

b) Limit Analysis of Notched Specimen under Tension

To analyze the V-notched tension specimens and

those with semi-circular notches used in the experimental investigation the classical method of Chapter I will be used. Mises yield criterion and associated flow law are assumed.

To determine a lower bound consider the rectangular tension specimen as shown in Figure 12 with a notch of half angle α, length $2lw$, and width $2w$. Then results may be extended to circular notches.

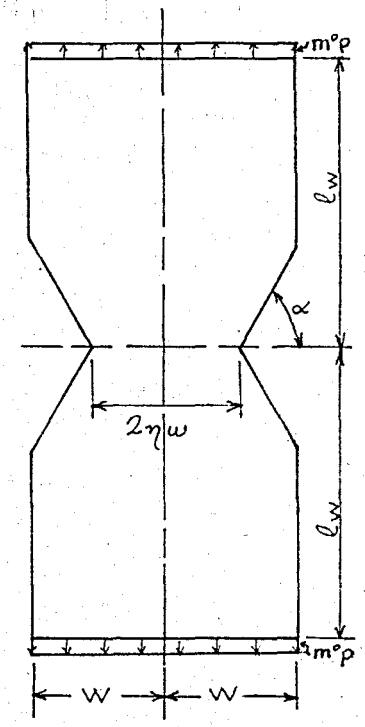

Figure 12 - Notched tension specimen

A stress field consisting of different regions of constant stress, seperated by lines of discontinuity will be assumed. The side of the notch makes an angle β with the vertical. The parameter $\lambda\omega$ determines the extent of region 3 as shown in Fig. 13. Because of the symmetry only one quarter of the specimen will be considered.

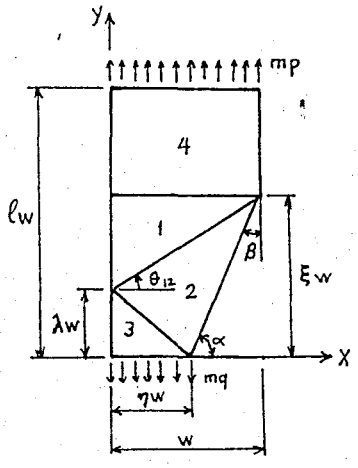

Figure 13
Zones of constant stress field in first quadrant

The following stress transformations are made (24) for sake of simplifying yield criteria, and reduce the numerical work.

$$\sigma_\theta = a - b\cos 2(\theta - \alpha)$$
$$\tau_\theta = b\sin(\theta - \alpha) \qquad (2.7)$$

where

$$a = \frac{\sigma_x + \sigma_y}{2}$$
$$b = \left[\tau_{xy}^2 + \frac{(\sigma_x - \sigma_y)^2}{4}\right]^{\frac{1}{2}}$$
$$\alpha = \frac{1}{2}\arctan\left\{\frac{2\tau_{xy}}{(\sigma_x - \sigma_y)}\right\} \qquad (2.8)$$

The positive direction of the stress compnents σ_x, σ_y, τ_{xy}, σ_θ, τ_θ and the angle θ are defined in Figure (14).

Stress components may be written as

$$\sigma_x = a + b\cos 2\alpha$$
$$\sigma_y = a - b\cos 2\alpha$$
$$\tau_{xy} = b\sin 2\alpha \qquad (2.9)$$

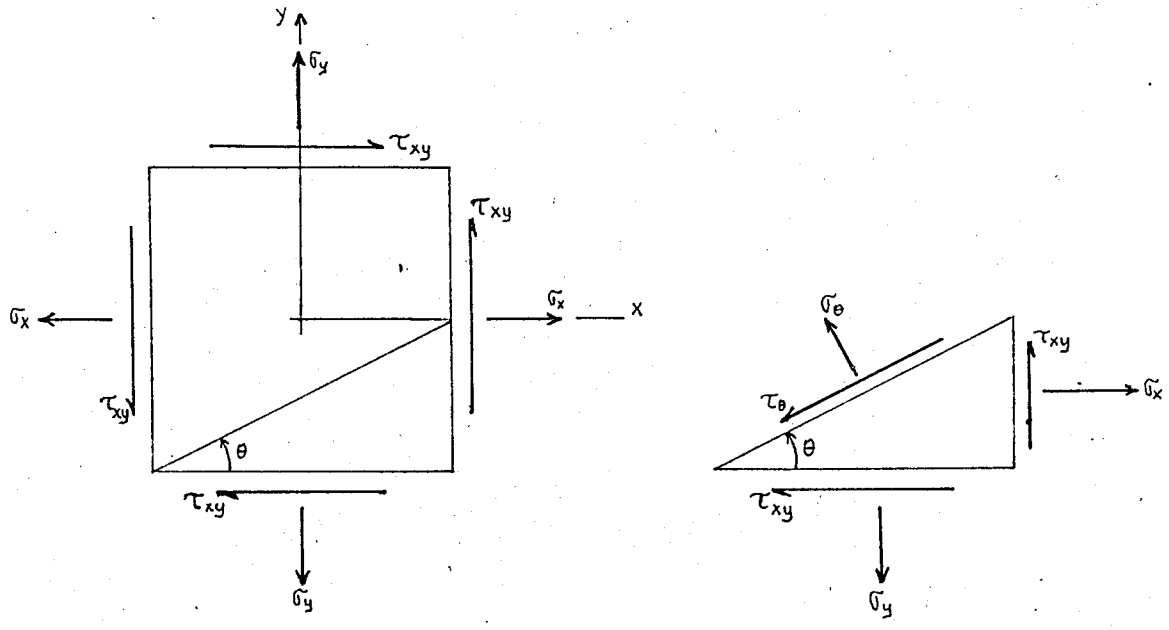

Figure 14
Defination of Positive Quantities in Stress Transformation

The exact location of various regions is determined by two redundant parameters β and λ. Choosing β and λ three stress parameters are determined from the boundry condition, and equilibrium conditions at lines of discontinuity (24). It can be easily seen that region 4 has only tensile stress of magnitude $m^o p$ which actually is the external load applied to region 1.

The unknowns, nine stress parameters plus q, the intensity of the tensile stress along x-axis which becomes part of the boundry when a quarter of the specimen considered are determined from three boundry conditions and the two lines of discontinuity each providing two conditions.

The following stress parameters for regions 2, 1 and 3 are then obtained (24):

$$\alpha_2 = \frac{\pi}{2} - \beta$$

$$b_2 = \frac{-m^o p}{\left[(\xi - \lambda)\sin 2\beta - \cos 2\beta - 1\right]}$$

$$a_2 = b_2$$

$$\alpha_1 = \frac{\pi}{2}$$

$$b_1 = b\left[\cos 2B + \left\{1 - \left(\frac{\xi}{\lambda} - \lambda\right)^2\right\}\frac{\sin 2\beta}{(2\beta - 2\lambda)}\right]$$

$$a_1 = m^\circ\rho - b_1$$

$$\alpha_3 = \frac{\pi}{2}$$

$$b_3 = b\left[\cos 2B - \frac{(\eta^2 - \lambda^2)\sin 2B}{2\lambda\eta}\right] \qquad (2.10)$$

$$a_3 = \frac{m^\circ\rho}{\eta} - b_3$$

The tenth unknown q being eliminated. For region 4 since $\sigma^\circ_y = m^\circ\rho$ and $\sigma^\circ_x = \tau^\circ_{xy} = 0$, we obtain:

$$\alpha_4 = \frac{\pi}{2}$$

$$b_4 = \frac{m^\circ\rho}{2}$$

$$a_4 = \frac{m^\circ\rho}{2} \qquad (2.11)$$

Those last twelve equations determine the stress field in the specimen in terms of the parameters λ. They satisfy the equilibrium and the boundry conditions. For this stress field to be statically admissable it must satisfy the yield criterion which in terms of (a) and (b) takes the form

$$\frac{1}{3}\left[a^2 + 3b^2\right] - k^2 \leq 0 \qquad (2.12)$$

assuming that plastic flow starts, taking the equal sign in Eq. 2.12 at certain regions, the unknowns λ and m° are found. The lower bound is found to be

$$m^\circ = \text{Constant}\ \frac{k}{\rho} \qquad (2.13)$$

CHAPTER III

PREPARATION OF SAMPLES

3.1 Machining - Material and Specimen

The specimens in this test program were machined from single pieces of commercial ST-37 steel bars having a nominal cross-section of 5 x 35 mm and a length of 600 cm. This is a Turkish variety of mild steel.

The intentionwas that all specimen have the same gross width of 35 mm and net width of 20 mm. Special attention was paid in locating the notches symmetrically. Very sharp tools were used, and to minimize the effect of work-hardening rather light cuts were taken. However a slight variation in net width and in thickness was unavoidable. Tables 1 and 2 show the dimensions and net cross-sectional areas for each individual specimen.

3.2 Heat Treatment

To miminize the further effect of machining (25), all samples were process annealed (26) in a controlled-atmosphere furnace for 60 min at 700°C and cooled to 230°C in 18 hours. In order to prevent the oxidation of samples during annealing they were put into specially prepared boxes and covered up with extra charcoal.

3.3 Hardness Test

Hardness tests were carried for each specimen after annealing to secure the uniformity of the samples. The resulting hardness after annealing was 59 to 63 Rockwell B. Sufficient readings were taken around the notches and samples outside the specified range were discarded. The results are recorded in Tables 1 and 2.

3.4 Designation of Specimen

Samples were cabagorized according to the series of tests to be performed, All V-notched samples were designated with letter

TABLE 1 : Geometrical properties and hardnesses of test specimens.

Designation	Angle of Notch	Hardness	Thickness cm	Net Width cm	Gross Width cm	Area	
						cm^2	in^2
V01		61	0.53	2.00	3.5	1.060	0.1635
V02	0	61	0.53	2.00	3.53	1.060	0.1660
V03		61	0.535	1.95	3.55	1.043	0.1615
V301		59	0.53	2.02	3.52	1.072	0.1665
V302	30	61	0.53	2.00	3.48	1.060	0.1642
V303		62	0.54	2.00	3.53	1.080	0.1672
V601		60	0.52	1.983	3.51	1.040	0.1600
V602	60	62	0.535	2.00	3.51	1.070	0.1657
V603		63	0.53	2.02	3.53	1.070	0.1660
V901		60	0.53	1.995	3.55	1.055	0.1625
V902	90	62	0.53	2.00	3.53	1.060	0.1642
V903		63	0.53	2.02	3.60	1.070	0.1660
V1201		61	0.535	1.99	3.55	1.045	0.1625
V1202	120	61.5	0.535	2.00	3.50	1.065	0.1657
V1203		61	0.53	2.02	3.54	1.070	0.1660
V1501		60	0.52	2.00	3.51	1.040	0.1611
V1502	150	61	0.52	2.01	3.53	1.040	0.1635
V1503		59	0.53	2.00	3.50	1.060	0.1641
V1701	170	63	0.55	1.98	3.50	1.080	0.1690
1		61.5	0.53	2.00	2.00	1.060	0.1642
4	0	60.5	0.53	2.03	2.03	1.076	0.1666
6		59.5	0.50	2.00	2.00	1.000	0.1548

TABLE 2 : Geometrical properties and hardnesses of test specimens.

Designation	Hardness	Thickness	d_1* cm	d_2* cm	Net Width d_1+d_2 cm	Area	
						cm^2	in^2
C1	60	0.52	1.03	1.08	2.11	1.095	0.1695
C2	60	0.52	1.04	1.06	2.10	1.092	0.1692
EA1	59	0.52	0.90	1.06	1.96	1.020	0.1580
EA3	63	0.53	0.88	1.09	1.97	1.045	0.1620
EB1	59	0.52	0.68	1.31	1.99	1.035	0.1605
EB2	59	0.54	0.60	1.43	2.03	1.095	0.1696
EC1	61	0.53	0.57	1.43	2.00	1.060	0.1642
EC3	60	0.52	0.54	1.52	2.06	1.072	0.1660
S3	60	0.52	--	--	2.01	1.045	0.1620
S4	62	0.52	--	--	2.00	1.040	0.1610
Sq1	59	0.52	0.96	0.98	1.94	1.010	0.1565
Sq2	61	0.51	1.01	1.03	2.04	1.040	0.1610
P1	60	0.52	1.01	1.02	2.03	1.055	0.1635
P2	59	0.48	0.98	1.02	2.00	0.960	0.1488

* d_1 and d_2 are shown in the figure.

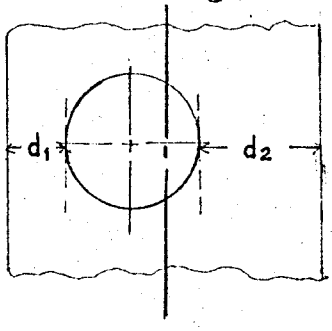

V, followed by numbers the last one being the sample number for specific angle and the remainder indicating the notch angle. For example V1201 indicates first sample of 120° V-notched series.

A square, a parallelogram, a circle at the center of the specimen, and a semi-circular notch symmetrically located from the centerline at the edges constituted the second series of experiments. The designation for this series is Sq. for square, P for parallelogram C for circular shape and S for semi-circular notch. Those were followed by specific sample number belonging to the same shape.

Eccentrically located circular shapes constitutes the third set of samples to be tested. They are designated by letters EA, EB, and EC where E indicates to eccentricity, and A, B, C refers to the different eccentricities, A being the smallest and C being the largest eccentricity. Figs. 15 and 16 show the three series.

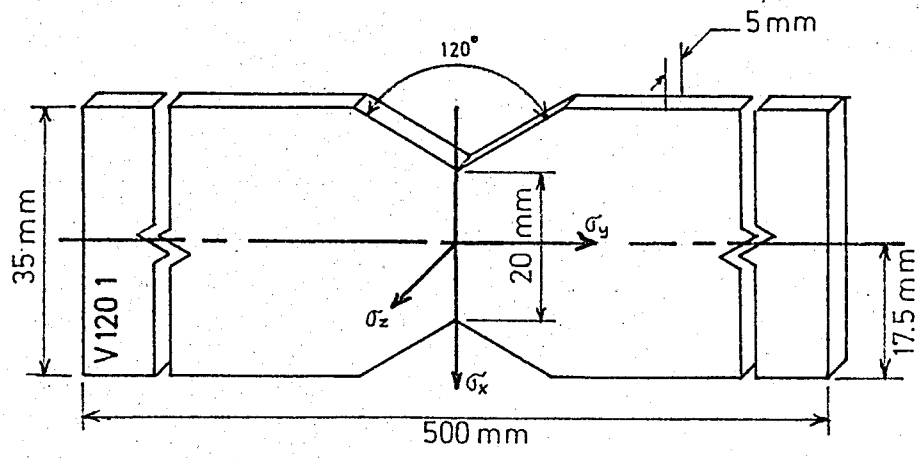

A V-Notched Specimen of 120°

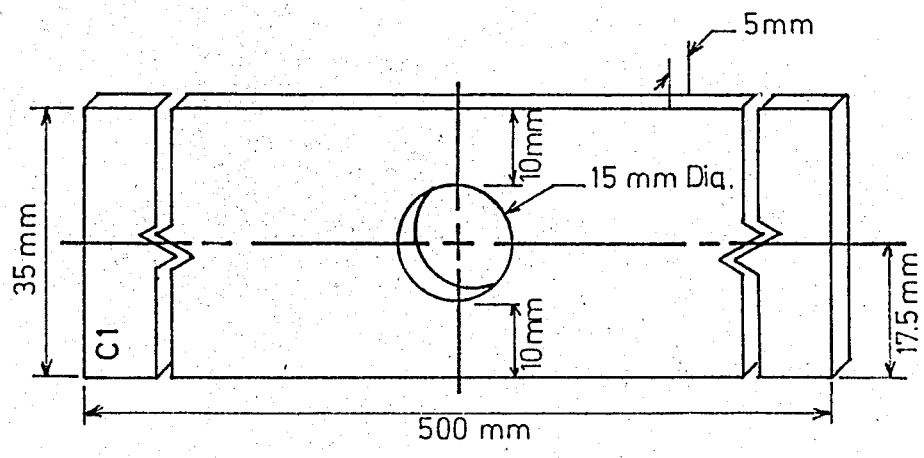

A Specimen With a Circular Hole at the Center

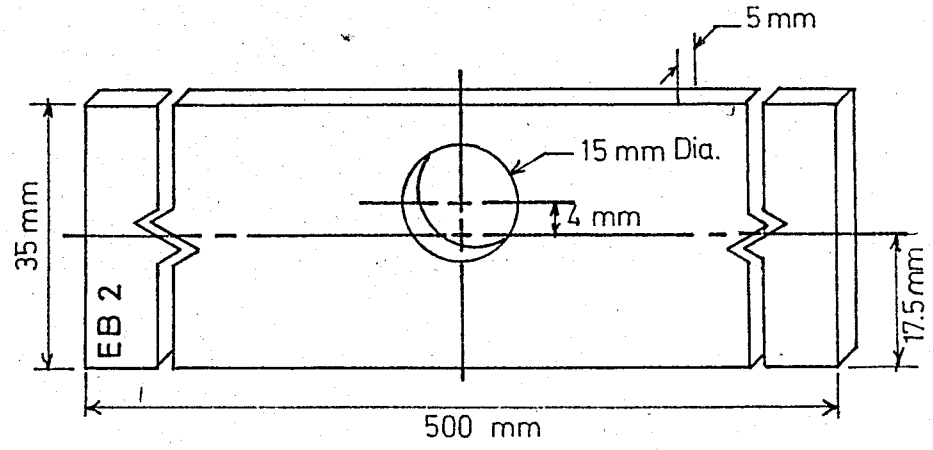

A Specimen With an Eccentrically Located Hole

Figure 15 Test Specimens

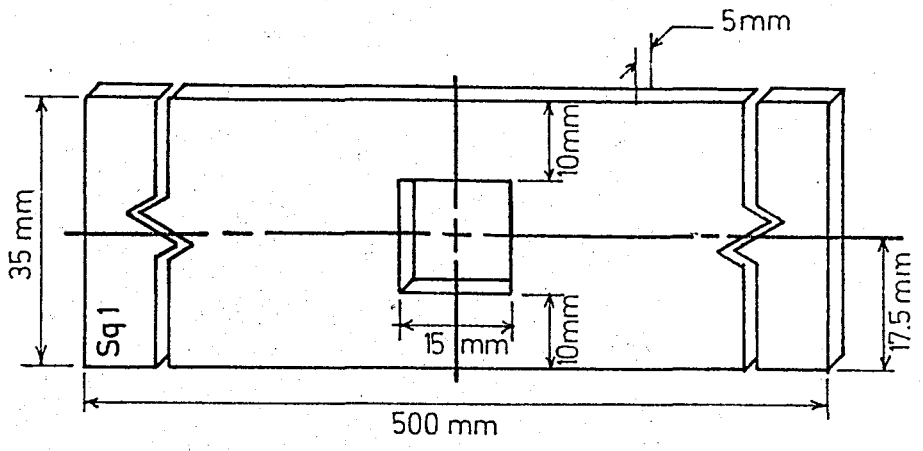

A Specimen With a Square Hole

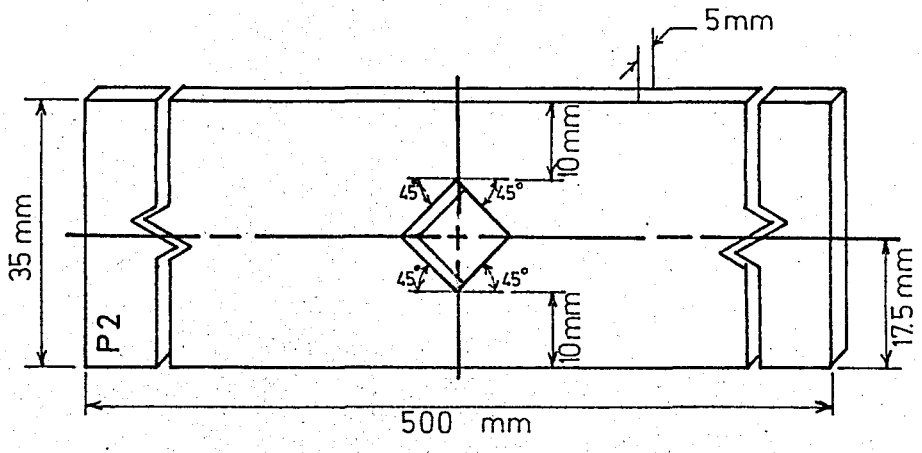

A Specimen With a Parallelogram Hole

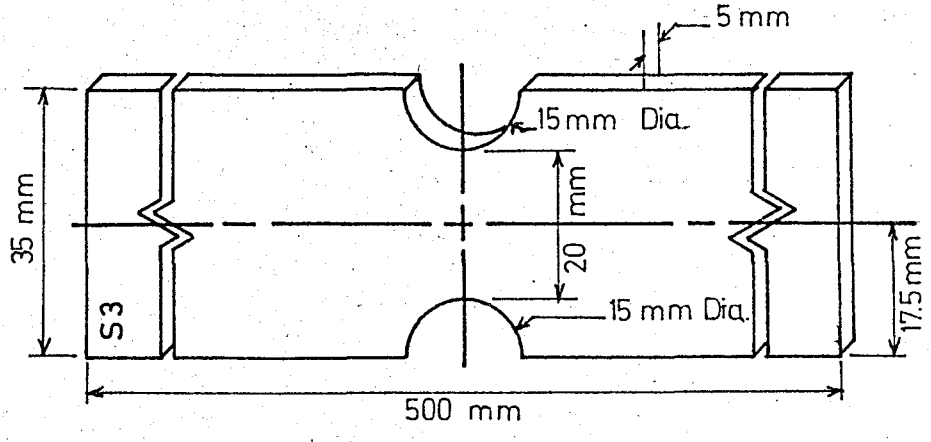

A Specimen With a Semicircular Notch

Figure 16 Test Specimens

CHAPTER IV

TESTING OF SAMPLES

4.1 Testing Apparatus.

The testing apparatus consists of the following:

a) Lever type testing machine with grips to fit specimen (Fig. 17). Type : Riehle

b) Strain gage of mechanical type with 0.0001" division and 2-in gage length (Fig. 18). Type: Riehle

c) Different types of SR-4 gages, basically A-1 A-5, A-7, AB-11 and SR-4 strain indicator bridge unit and SR-4 switching and balancing unit (Fig. 19). Type: N, Baldwin-Lima-Hamilton

d) Miscellaneous small items

4.2 Technique of Mounting an SR-4 Gage

Following the directions furnished by the manufacturers cataloque surface of the specimen where gage were to be attached to was thouroughly cleaned first by rough sand paper followed by No 1,No. O and OO finest quality sandpapers. The samples were further cleaned by either carbon-tetra-chloride, or acetone. No. OOO sandpaper was then used for roughening the surface. 404, a commercial cement was used for three samples, the results obtained weren't successful. Therefore Duco-Cement was provided and used for attaching the SR-4 gages. After gages have been attached to the sample, a rubber was placed on each gage which was further loaded by a weight of about one pound. When, the cement became sticky, usually after 30 minutes, weight and rubber were carefully removed. All the samples with attached gages were left to dry for at least 50 hours before soldering copper wires to the gage terminals. While soldering, special care was taken so as not to damage the gage.

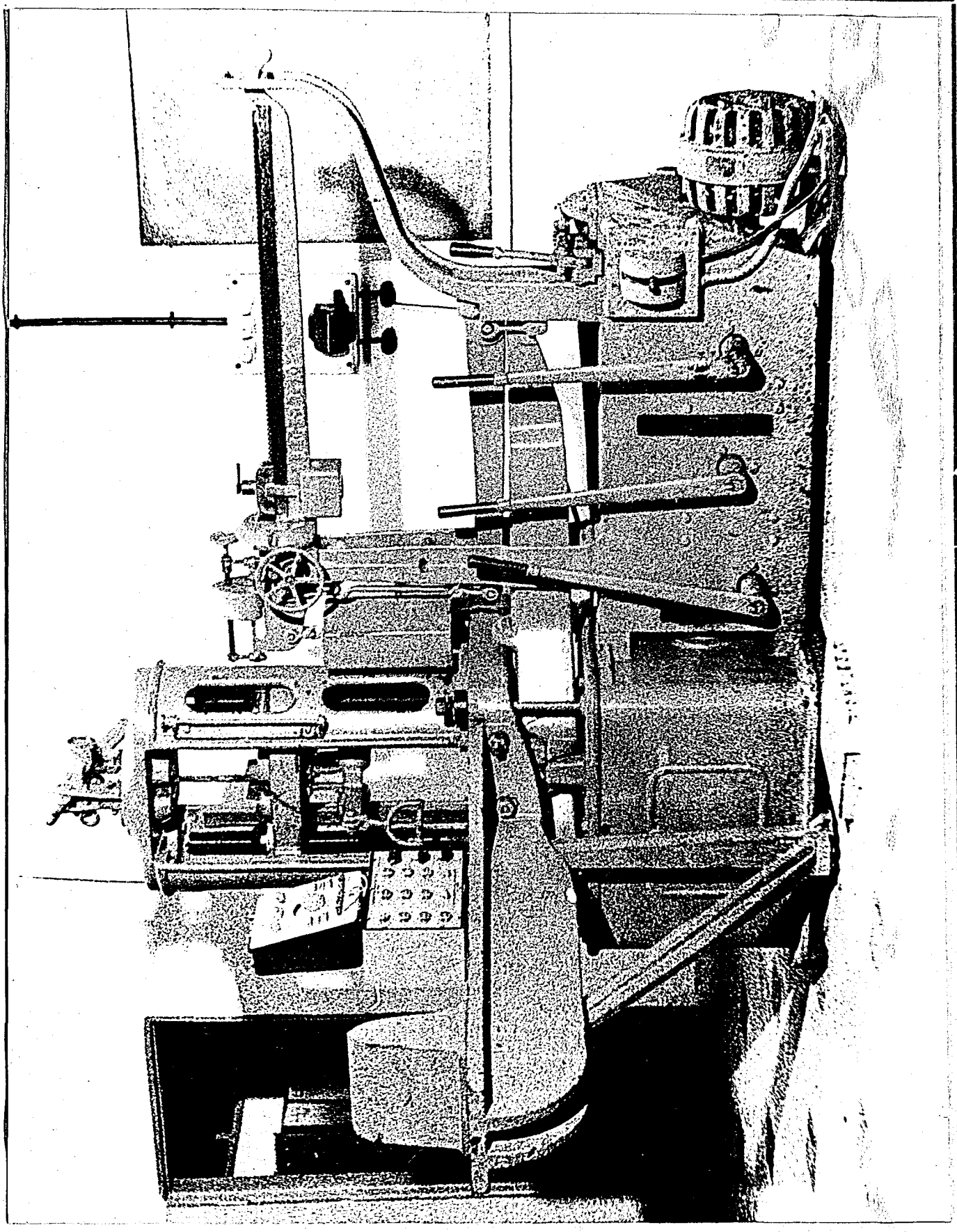

Figure 17

Testing Machine

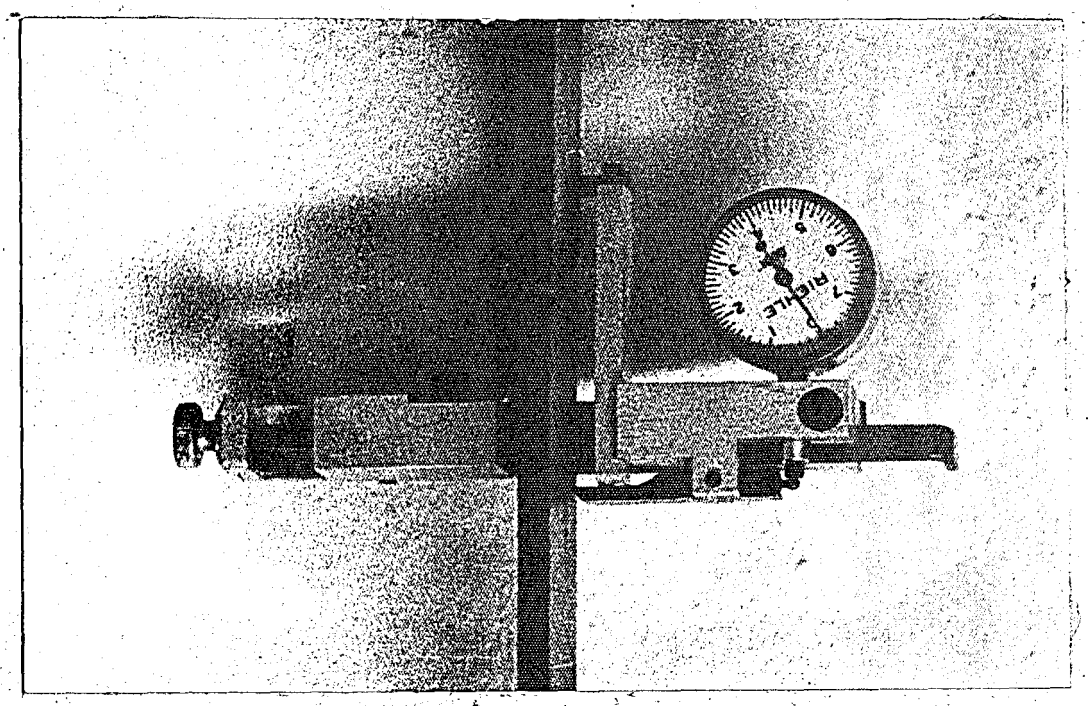

Figure 18
Mechanical Strain Gage

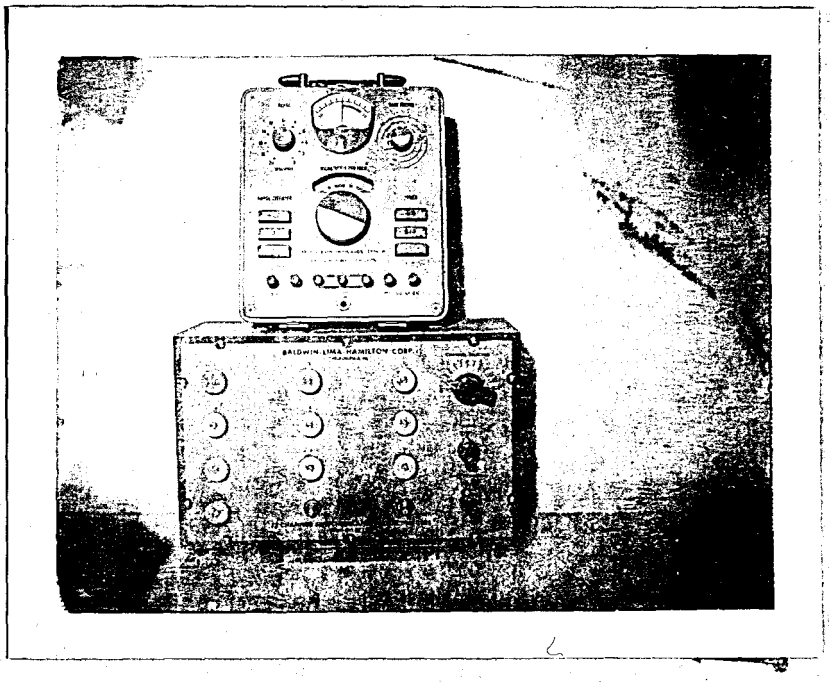

Figure 19
SR-4 Strain Indicator and switching and balancing unit.

4.3 A Brief Summary of Electric Strain Gages

a) Description of Performance

Mechanical strain gages are used to magnify the strain mechanically till it can be perceived by the eye. However, it is inescapable that one of the weak points in a mechanical strain gage is the problem of undistorted amplification of the strain. A somewhat less direct method is to; a) translate the strain into some electric property change such as resistance, the inductance, the output voltage or the capacitance by use of transducers or translating device. They maybe of variable resistance, variable inductance, variable-capacitance, piezoelectric or photoelectric types; b) amplify this change electrically and; c) retranslate the electric change back into one of length, generally by making a pointer move along a calibrated scale or cathode-ray trace move on an oscillograph screen (13).

When an electric strain gage is used, the amplification of an electric quantity can be easily performed with a minimum of distortion, and particularly with no limit to sensitivity.

b) The Variable-resistance Strain Gages

The most common of all is SR-4 * bonded-wire resistance gage. The SR-4 strain gage consists of a grid of very fine wires of a copper-nickel or other suitable alloy, arranged as shown in Fig. 20 (14). Two heavier wires serve merely as terminals for electric connection. The grid may either be bonded to a paper base or to a Bakelite base. The latter has the advantage for use in higher temperature locations, and under extreme conditions of humidity. (13)

When SR-4 gage is attached to a specimen as the length of that specimen changes, the length of each long fine wire will also change- (assuming that cement does not suffer shear deformation). This change in wire length will result in a decrease or an increase between two terminals of the gage, and by suitable devices the

*The trade name SR-4 comes from the initials Simons and Ruge who

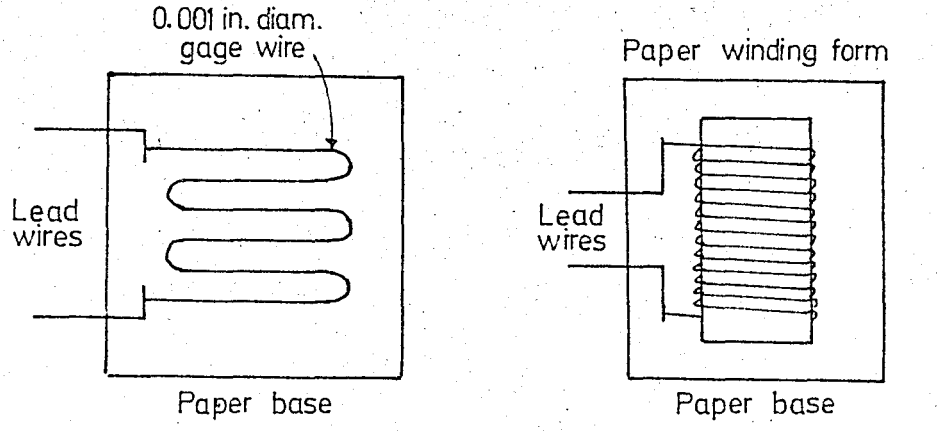

Figure 20

Bonded-Wire Strain-Gage

magnitude of any change in strain is detected.

c) SR-4 Temperature Compensation

A change in the temperature of the wires of the SR-4 gage will also change electric resistance. In order to compensate for this change, a dummy gage with the same lot number is attached to the unstressed piece of the same material, in the same manner, with the same protective coating as the measuring gage.

d) Gage Factor

The actual change in electric resistance of the fine wires upon being strained is actually greater than that due solely to change in length alone. Because as the length of the wire is increased, its cross-sectional area will decrease. Increase in the length and decrease in the cross-section both contributes to the change in electric resistance. The decrease in area is accounted for by a "gage factor", which is experimentally determined by the manufacturer of the gage.

---

* (cont) perfected the gage, and that there were four men involved in its commercial development.

The gage factor also accounts for the "loop effect" or "transverse sensitivity".

e) Electric Resistance Measurements

The most common method of measuring electri-resistance values and any change in electric resistance is by use of a bridge circuit, such as Wheatstone Bridge (Fig. 21).

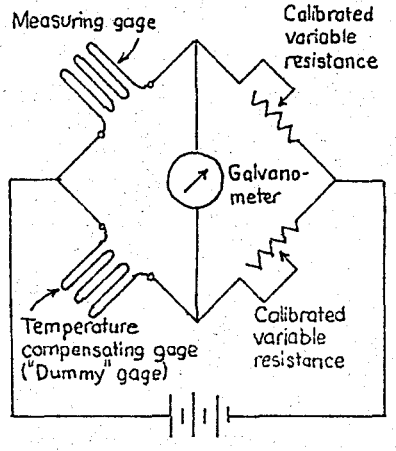

Figure 21
Wheatstone Bridge Circuit for SR-4 Strain measurement

If both dummy and measuring gages suffer same temperature change the bridge will be unaffected. First balancing is made by adjusting the calibrated variable resistances. After the gage has been strained a second balance is made by observing the Galvano-meter. With help of commercially available bridge units change in resistance is directly read as change in strain.

f) Selection of Gages

1. Gage Length

In using the strain gage it is usually assumed that the strain which acts upon that particular gage is constant over the active length of the strain gages. Therefore, for uniform stress cases gages of any length could have been used.

However, if the member is of complex form, where stress distribution may not be uniform, and change very much from point to point, the gaging length of the strain gage should be as short as is practical. SR-4 gages from several inches down to 1/10 inch gage lengths are available. For our tests A-1, A5 gages were used for uniform stress conditions.

2) Gage Width

Due to the reasons stated above, effective width of a strain gage will also be factor in gage selection, since any strain measurements will be averaged over both length and width of the gaging area. Gages having width of less than 1/8 inch are available. In this work, AF-7 and A-12 gages were used, especially for EA, Eb, Ec, Sq and P series of samples.

4.4 Brittle Coating Technique

The term "brittle coating" is used to describe a coating which will fail or crack when a certain value of tensile stress is exceeded without an appreciable yielding, or inelastic action preceding the actual cracking. The proper use of the brittle coatings, (stress coat) will graphically show the magnititude, direction, distribution and the gradient of the force on a real structure (27). Among the several important application of the stress coat three important ones can be counted. First, the crack pattern can be used to determine the best location for SR-4 strain gages. Second, an approximate value of stress indicated by the initiation of cracks at a particular load maybe used to redesign the member to reduce the stress around stress concentrations. Finally, stress-coat may give a better information at the stress concentration points where SR-4 gages aren't applicable.

The flaking of the brittle oxide scale on hot rolled steel acts as a stress coat and has been long recognized as an indication of "local yielding". See Figures 22, 23, 24 and 34. "Leuder's Lines" are the example of this (13). They are obtained experimentally by the tensile loading of hot rolled flat strip as shown in Fig. 24. If failure was just due to shearing, the lines would be inclined at

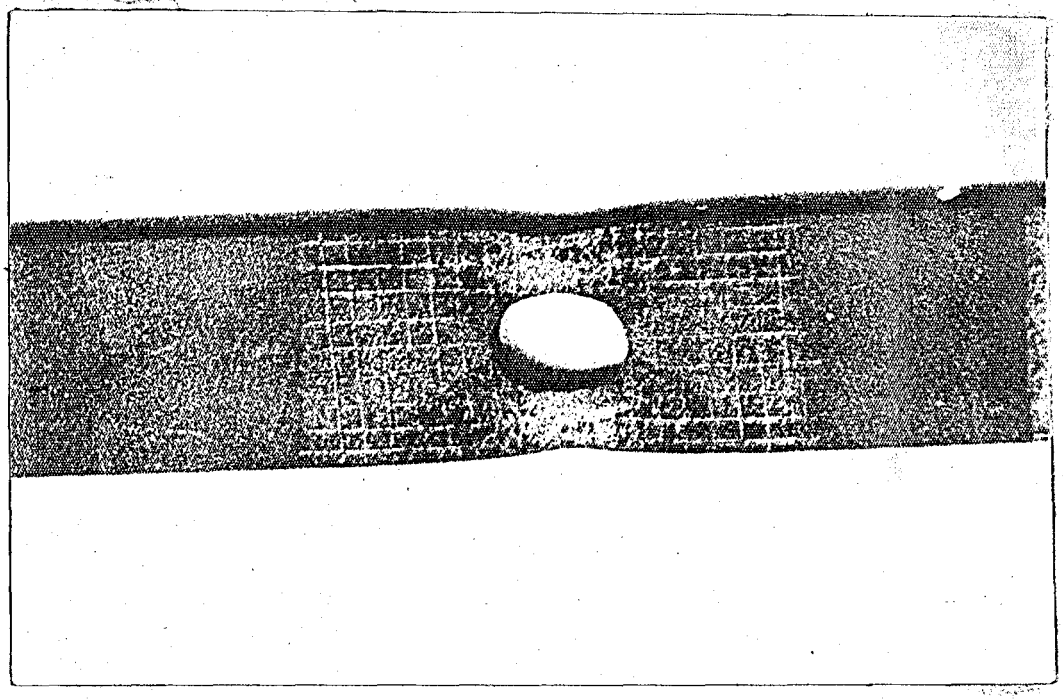

Figure 22
Flaking out of brittle lacquer.

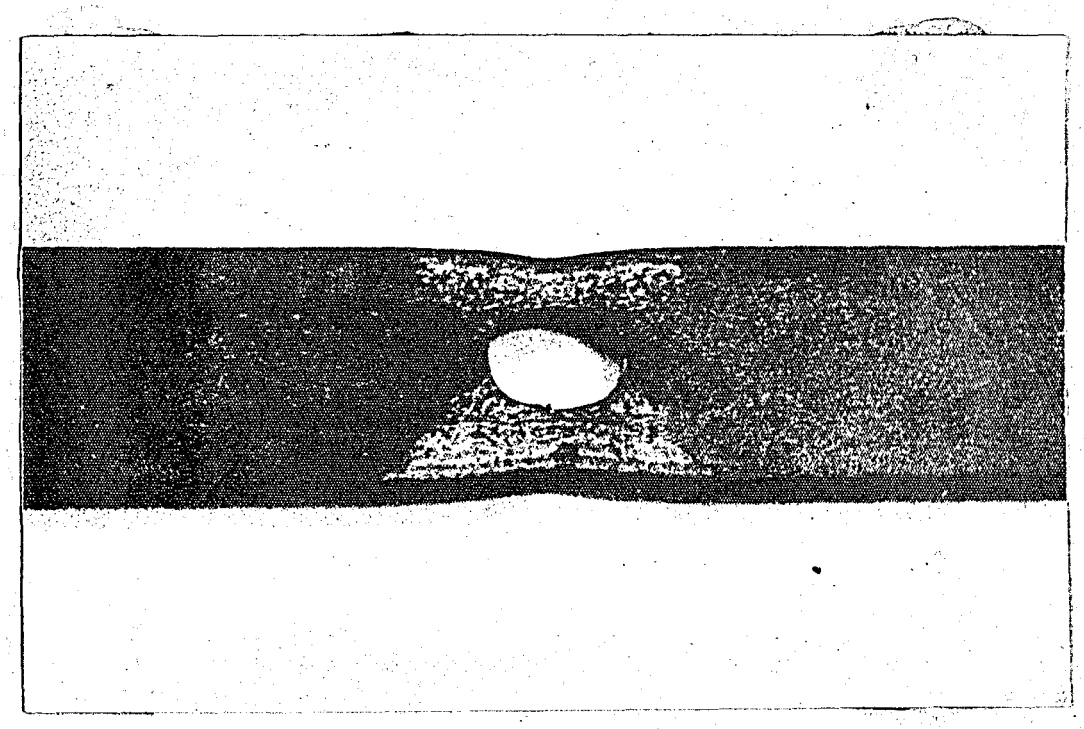

Figure 23
Flaking out of iron oxide coating.

45° to the axis of tensile loading.

Brittle lacquers are designed under the trade name "Stresscoat", to start to fail at varying strains about 0.0005 in/in to about 0.0015 in/in , depending upon temperature and humidity conditions during drying and testing.

In this experimental work, several samples were stress-coated and grid lines indicated were drawn on some of them in order to detect pattern of deformtion, or local yielding by flaking out of the lacquer. Results so obtained will be discussed in Chapter VII.

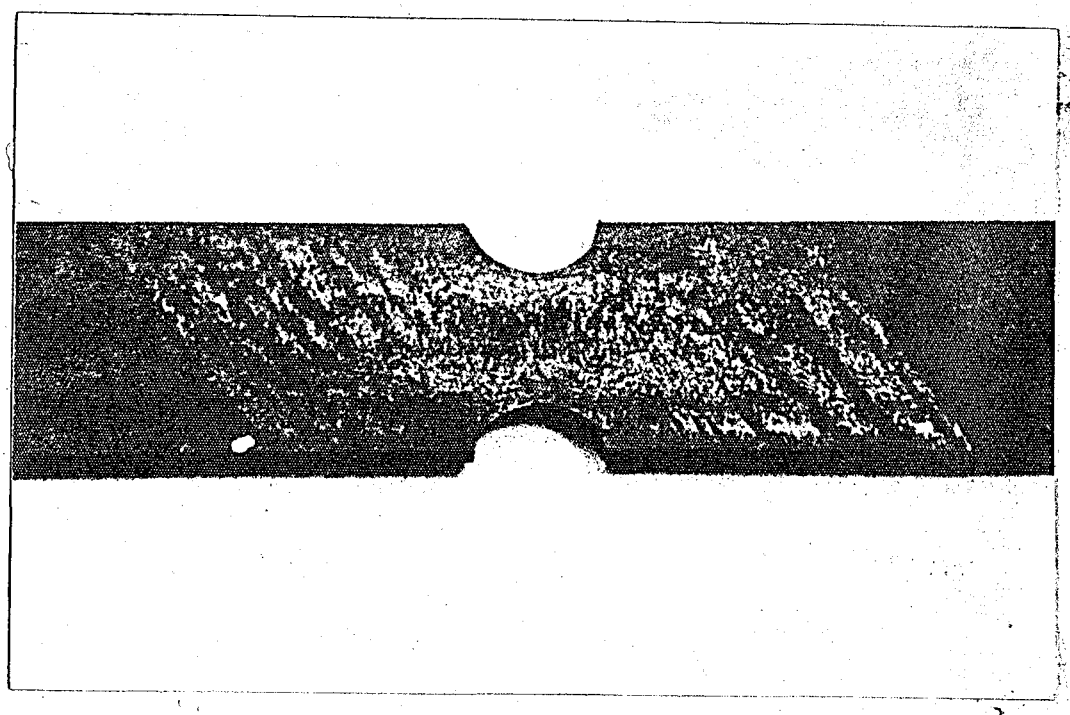

Figure 24
Picture showing flaking out of "brittle oxide coat" *

* It is interesting to note that angle that longitudual axis of the member makes with the leuders's lines - which are the slip-lines also, is roughly 45° .

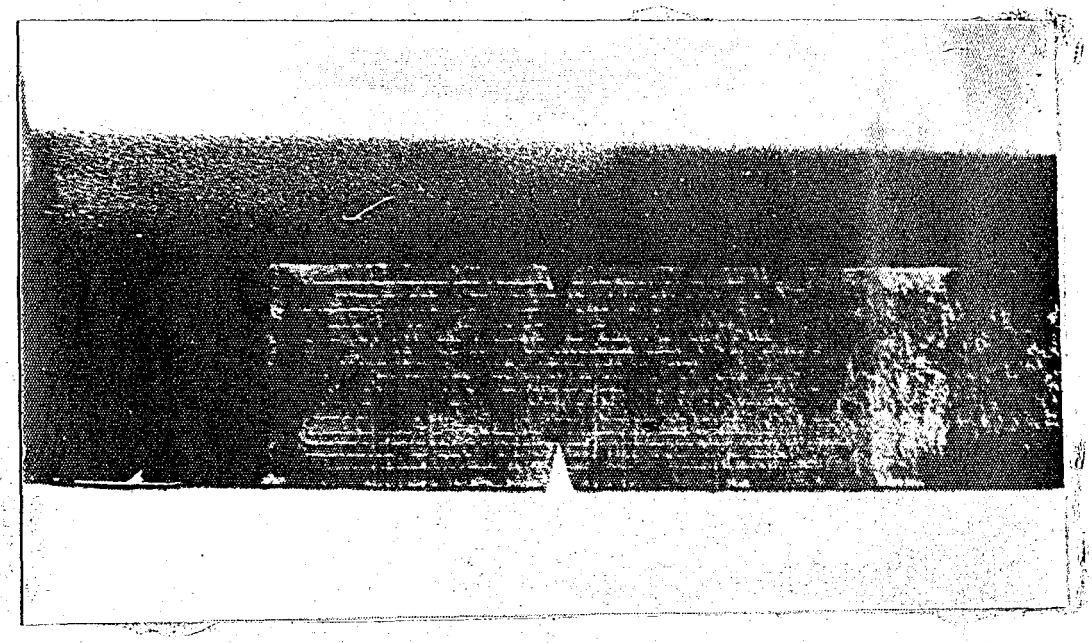

(a)

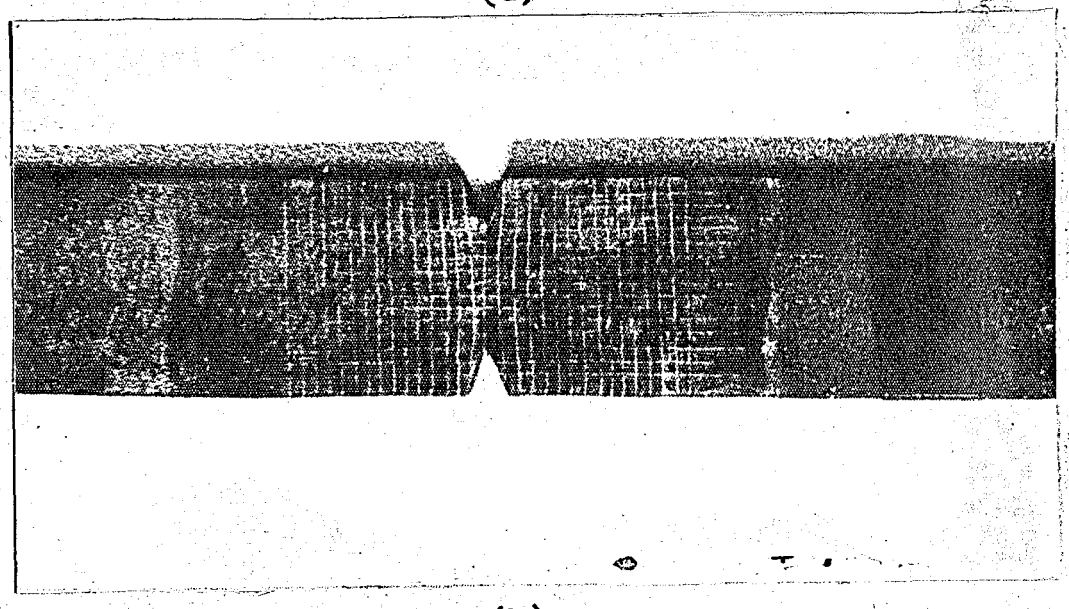

(b)

Figure 25

A stress-coated V-notched sample with grid lines

a) undeformed b) deformed

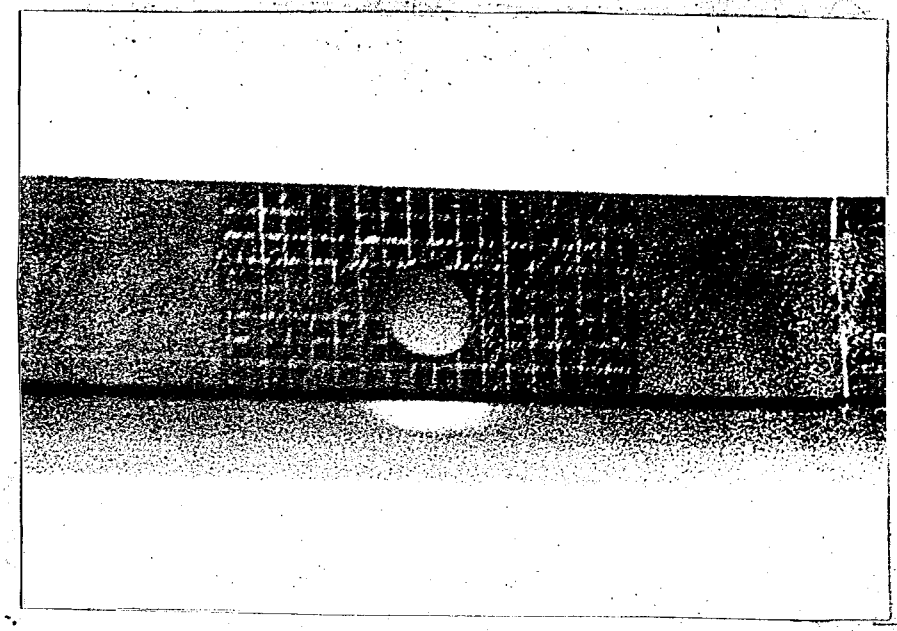

(a)

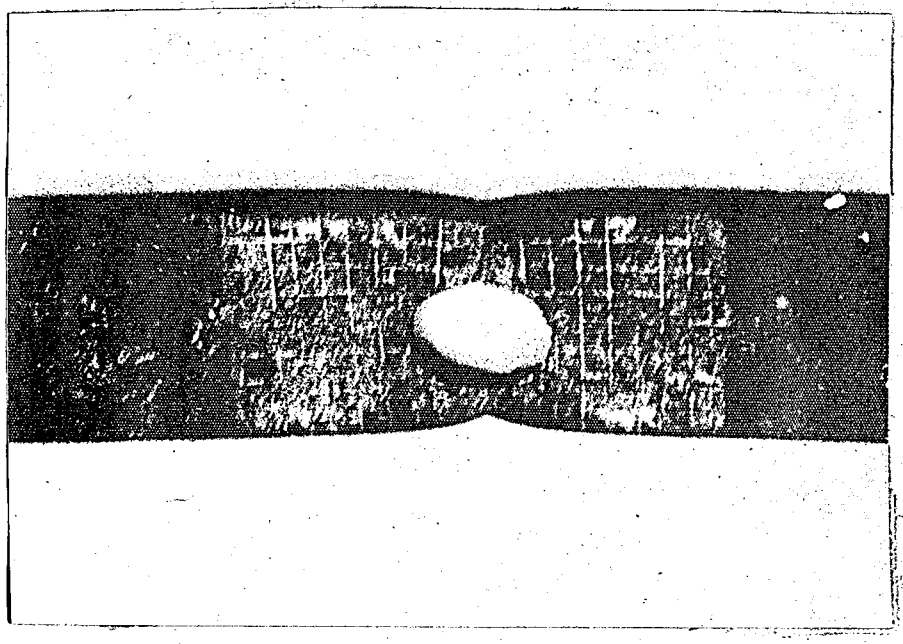

(b)

Figure 26
An eccentrically drilled and stress coated sample with grid-lines a) undeformed b) deformed and ruptured

4.5 Experimental Technique

A lever type (Fig.17) Richle testing machine of 70000lbs capacity may introduce errors in calculations of average stresses owing to the fact that an average cross-section of 0.1640 in^2, which the net cross section of the samples tested under a load of 100 lbs would be subjected to a stress of more than 600 psi . In order to secure maximum accuracy with such a machine, it would be stopped and no reading would be taken till the load had balanced. Mechanical strain gage of Riehle type (Fig. 18) with two-inch gage length seemed sufficient for reading average strain values over plane prizmatic bars with no notch. SR-4 strain indicator (Fig.19) worked very well due to a sensitivity of more than 1×10^{-6} in/in . However, close to the yield load, both balancing the load and keeping the reading of the strain indicator constant presented some problems. Although the slowest test rate (strain-rate) was secured in order to avoid getting a yield point higher than the actual (2), sometimes there had been a jump in load reading.

Bars with 180° notches (plane prizmatic bars) didn't come into plastic region although they were stretched to a great extent. The reason can be stated as follows: Since there was no change in the cross-section along the length of the specimen, no singular cross-section would enter into plastic region, unless a certain over-all elongation took place in order to cause plastic flow at a certain location.

The grips of the testing machine not being completely attached, introduced some eccentricity problems during the testing. While mounting the specimen on the testing machine maximum effort was spent in order to make it concentric. A test set-up is shown in Fig. 27.

Because of the constraint of the pulling system, non-uniformity of the lower yield point, and instability of upper yield point, readings around yield could have diverted from the actual values.

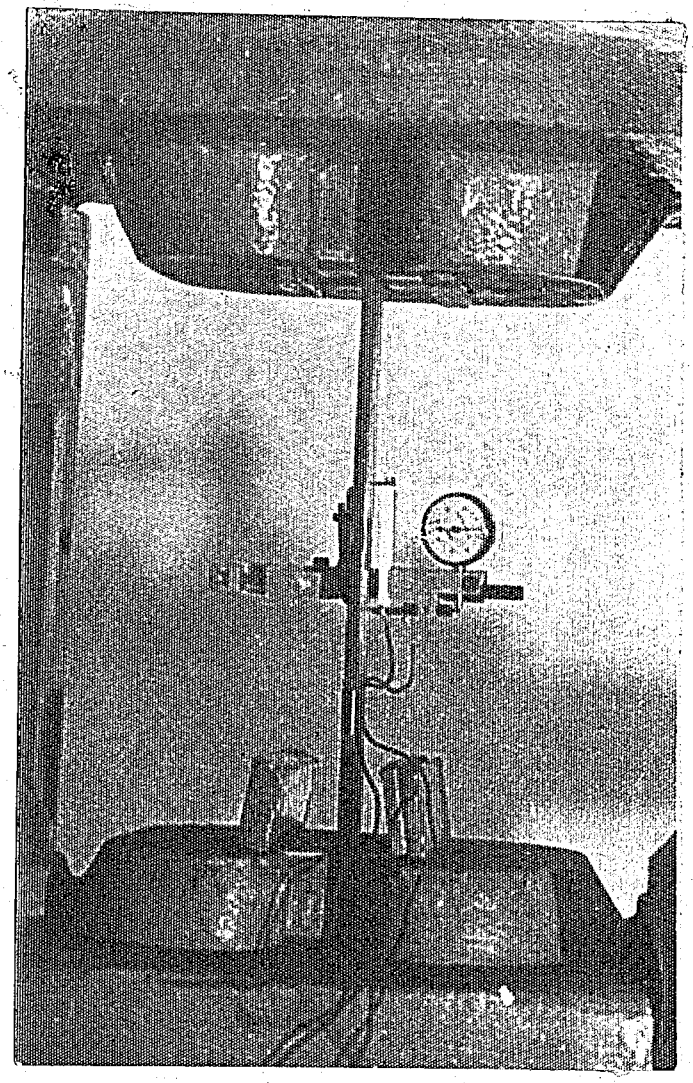

Figure 27
Test Setup

Leveling out of strain at yield, up to a point was prevented by the high stress concentration occuring at the corners of notch and redistribution of loads. As yield point was reached readings were taken after few minutes without applying additional load. Therefore uncertainity of upper yield point was avoided.

In some tests, bending was detected, and other samples of the same series were tested in order to get better results.

For bars with holes eccentrically located, two SR-4 strain gages were used. However, usually one would suffice together with a mechanical strain gage (Fig. 28).

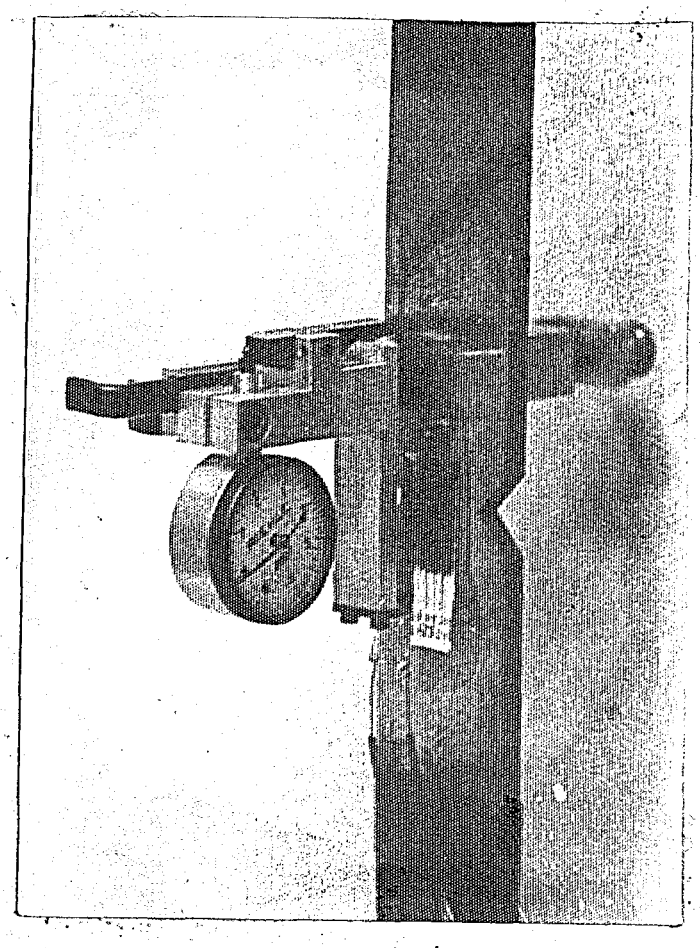

Figure 28
A V-notched specimen with mechanical strain gage and SR-4 gage attached

CHAPTER V

EXPERIMENTAL RESULTS

5.1 V-Notched Series

The experimental results obtained for the V-notched series indicate an obvious rise in the average stress of each speciment at the yield.(Fig. 29). The yield point of 180° notch is 36 ksi. This will be taken to be the yield stress σ_o .

The constraint factor is defined as $\frac{P}{\sigma_o A}$ where P is the load causing the material yield plastically, and A is the net cross-sectional area between the notch roots. Table 3 shows all the calculations pertaining to the average stresses and the constraints factors.

TABLE 3 : Experimental results of a V-notched series.

α	Sample Number	P/A (psi)	Average P/A (psi)	Constraint factor L
	1	41300		
0°	2	41200	41250	1.146
	3	41200		
	1	41400		
15°	2	41250	41400	1.150
	3	41500		
	1	41350		
30°	2	41300	41300	1.148
	3	41250		
	1	41250		
45°	2	41000	41000	1.139
	3	40750		
	1	41400		
60°	2	40000	40750	1.132
	3	40000		
	1	40300		
75°	2	41200	40650	1.130
	3	40500		
85°	1	39000	39000	1.056
90°	1	36000	36000	1.000
	4	36000		

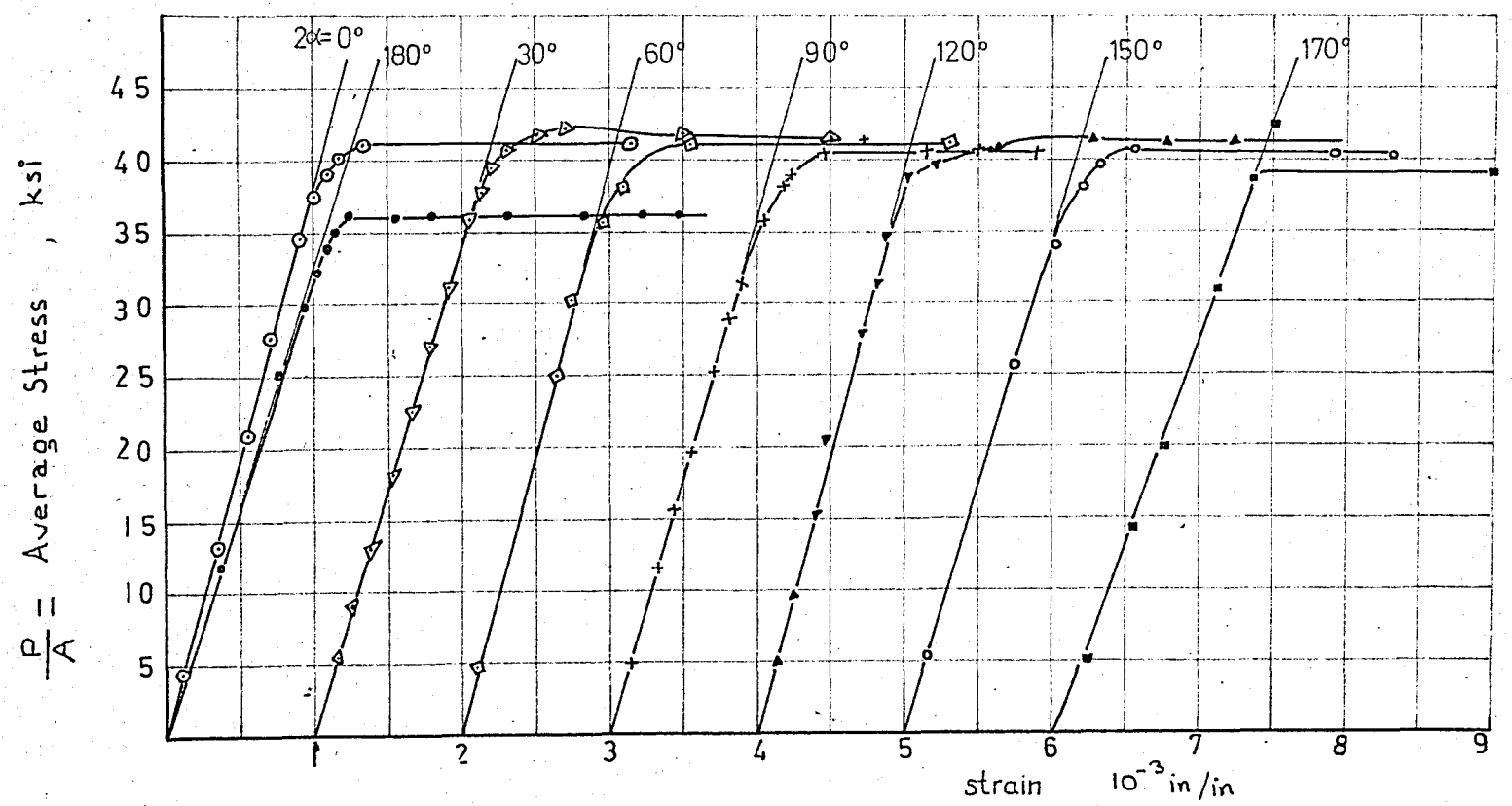

Figure 29. V-notched strips under tension

The constraint factors obtained are plotted together with their theoretical upper and lower bounds in Fig.30 against the parameter α, half angle of the notch. The lower bounds of the constraint factors are computed in Chapter VI. The upper bounds are taken from a solution given by Hill (28).

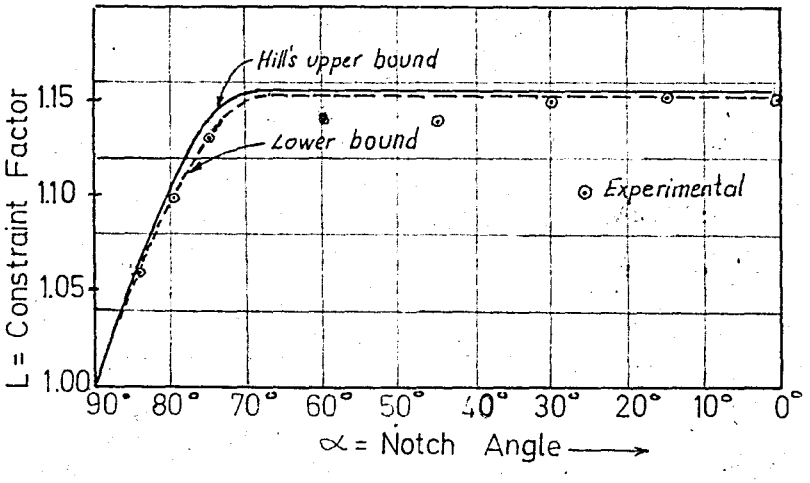

Figure 30
Constraint factor versus half the notch angle *

Experimentally the highest constraint factor obtained is for the specimen with a half notch angle of 15° . However values below or above this value are close enough to plot straight line up to $0 \leq \alpha \leq 70°$.

---

* The following changes had been made concerning Figure 30 :

1) A weighted average value for the specimen with half notch angle $\alpha = 60°$ has been used.

2) A hardness correction has been applied for the sample with $\alpha = 85°$, due to its rather higher hardness (65 Rockwell B, compared to 60-61 for the rest of the samples). The load that caused yielding (39,000 psi) was reduced by 2.5 % in Figure 30. The constraint factor L= 1.056 in Table 3 is the corrected value.

Various angles measured between the slip lines or Leuder's which conincide with the direction of maximum shear stress (14) and the longitudinial axis are between 47 to 55 degrees most of them averaging 50 degrees.

5.2 Holes of Various Shapes

The average stress P/A versus strains curves for various holes of different shapes, and semi-circularly notched specimens are presented in Fig. 31 . Semi-circularly notched specimen gives the highest value of P/A (average stress of 40 ksi), whereas square shaped specimen gave the lowest results, 34.5 ksi. However, since according to Mises criteria (21) an increase of 15 % would be expected for the semi-circularly notched specimen, result obtained is 3.27 % below that of theoretical value.

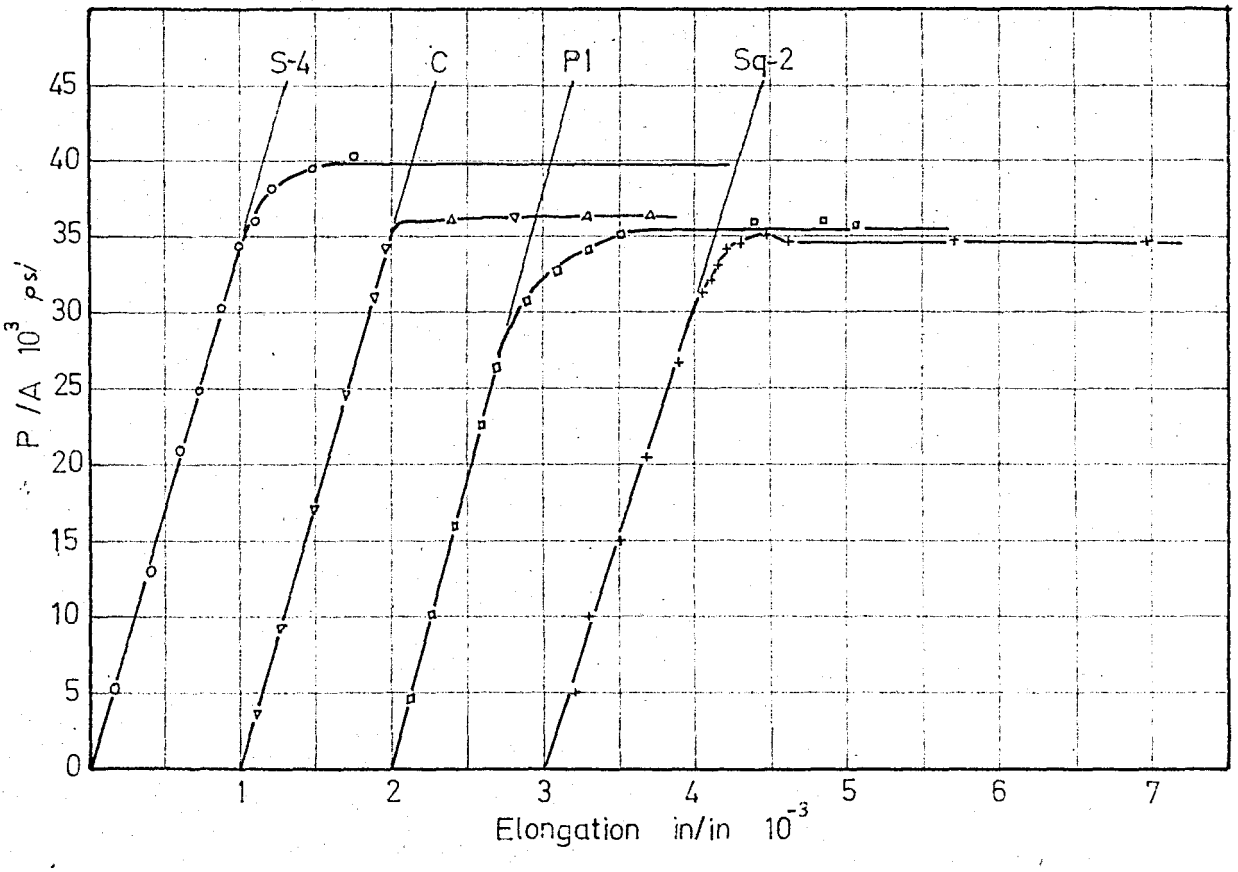

Figure 31
Strips with holes of various shapes under tension

The value of average stress of a concentrically located hole seemed to be about the same as the actual yield stress of the material. Table 4 gives a detailed account of the yield points and the constraint factors obtained. The average stresses at yield obtained for square and parallelogram cut-out are respectively about 11.6 % and 11.25 % lower than that of circular notched specimen.

TABLE 4 : Experimental results for strips with cut-outs.

Shape	Designation	P/A	Average P/A	Constraint Factor
Semicircular Notch	S3	40250	40000	1.111
	S4	39750		
Circular Hole	C1	36000	36000	1.000
	C2	36000		
Square Cut-out	Sq1	34250	34500	0.958
	Sq2	34750		
Parallelogram Cut-out	P1	35500	35500	0.986

Figure 33 and Figure 34 show the fully plastified zones around the each discontinuity. It is important to realize the idealization made by Drucker (21) such that around the discontinuity simple 45° rigid blocks motion is creadted, Fig. 32.

It can be concluded by observing Fig. 34 that four corners of the square cut-out are subjected to the same stress-concentration where as, it is the widthwise corners of a parallelogram, where the fracture begins.

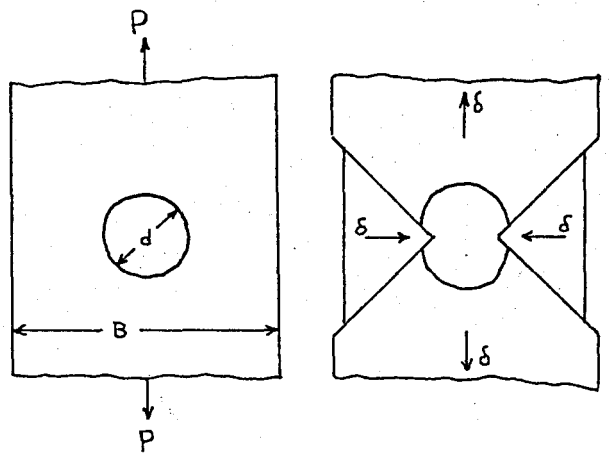

Figure 32
Plastic plane strain in the plastic range at plane stress loads.

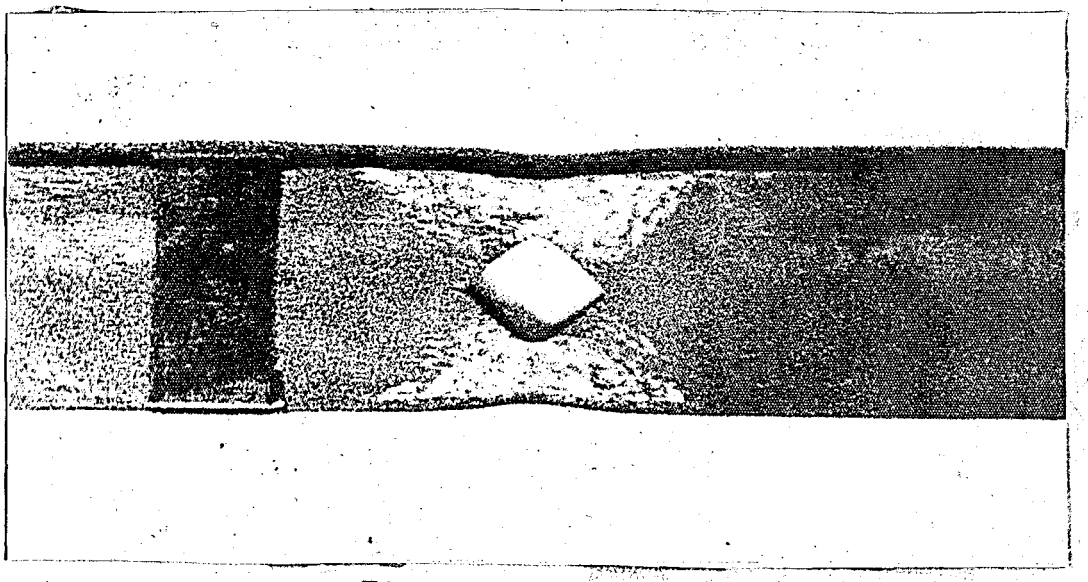

Figure 33
Plastified zones around a parallelogram hole

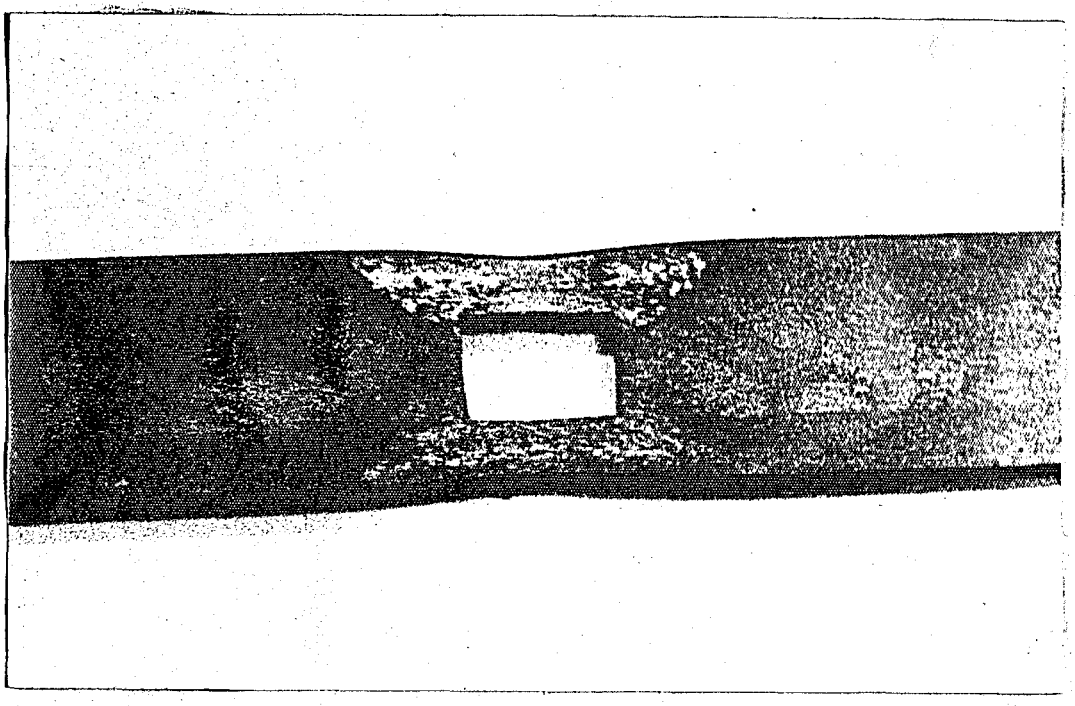

Figure 34
Plastified zones around a square hole.

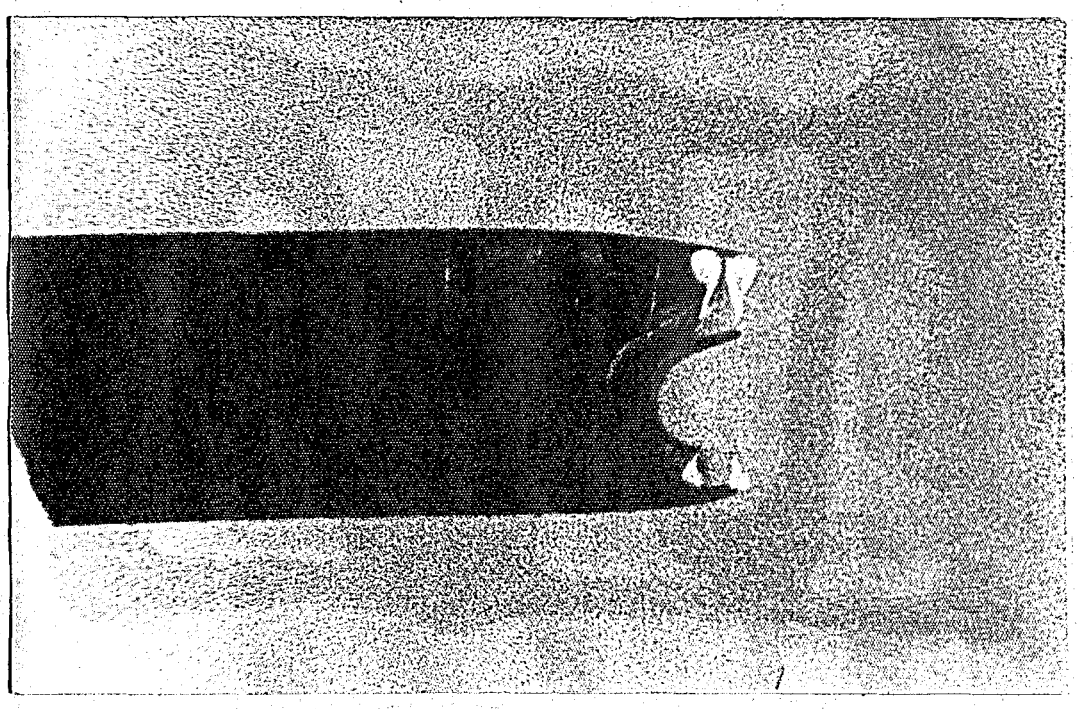

Figure 35
Fracture Pattern of a Tension Strip
with an Eccentric Hole

5.3 Eccentrically located Circular Holes

As it was stated in Chapter II, the possibility of locating a hole eccentrically is very big. The AISC Code (29), considering such effects of accidental eccentricity requires that a reduction of 15 % in the net area of a tension member to be made.

Stress versus strain diagrams are shown in Fig. 36 . The average stress versus average strain recorded at the bigger and smaller cross-sections are plotted.

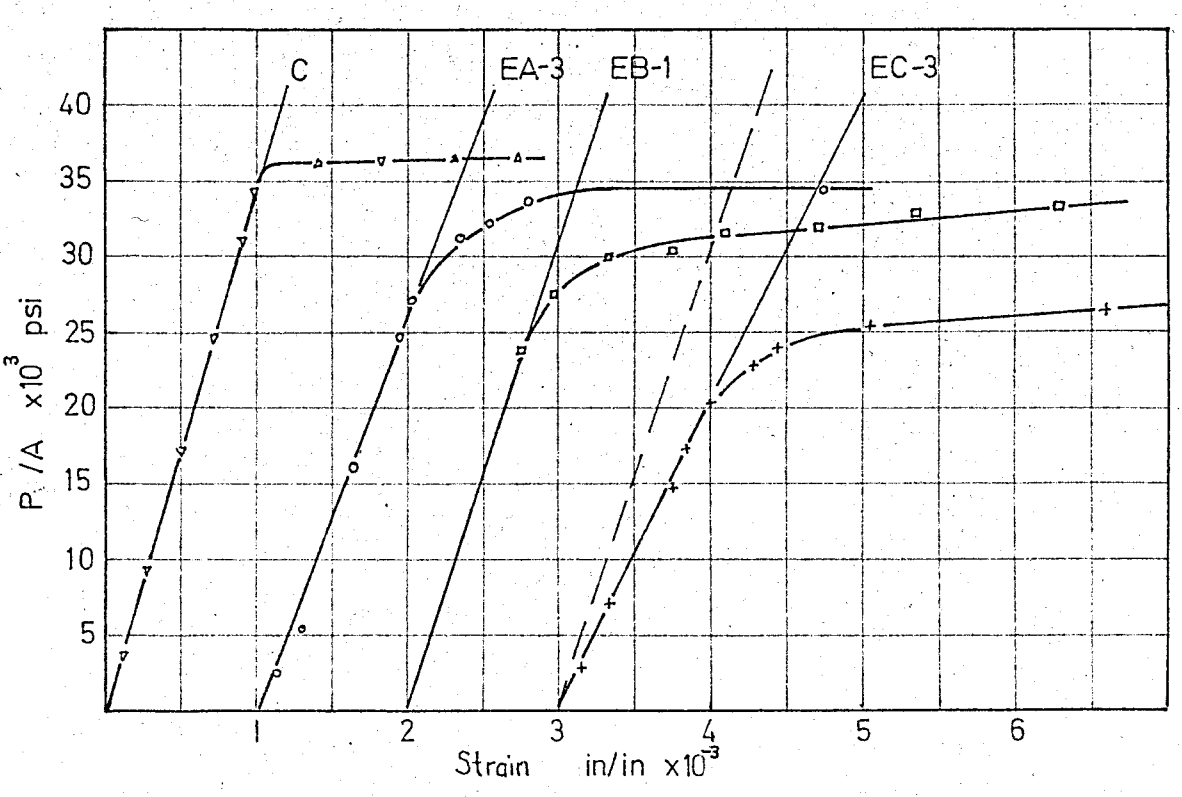

Figure 36
Strips with eccentric holes under tension.

The experimental results of tension members with eccentrically located holes shows that as eccentricity gets bigger (from 0 mm to 6 mm), the value of contraint factor goes down from 1.0 for zero mm eccentricity to 0.764 for 6 mm eccentricity, as shown in Table 5, values of contraint factors versus eccentricity are plotted in Fig. 37 . Fracture Pattern of a specimen with an eccentricity of 4 mm is shown in view 35.

TABLE 5 : Experimental results of strips with eccentric holes.

Eccentricity (mm)	Average Stress P/A (psi)	Constraint Factor
0	36000	1.000
2	34400	0.956
4	32000	0.889
6	26500	0.764

The variation of constraint factor with respect to eccentricity is shown in Fig. 37 .

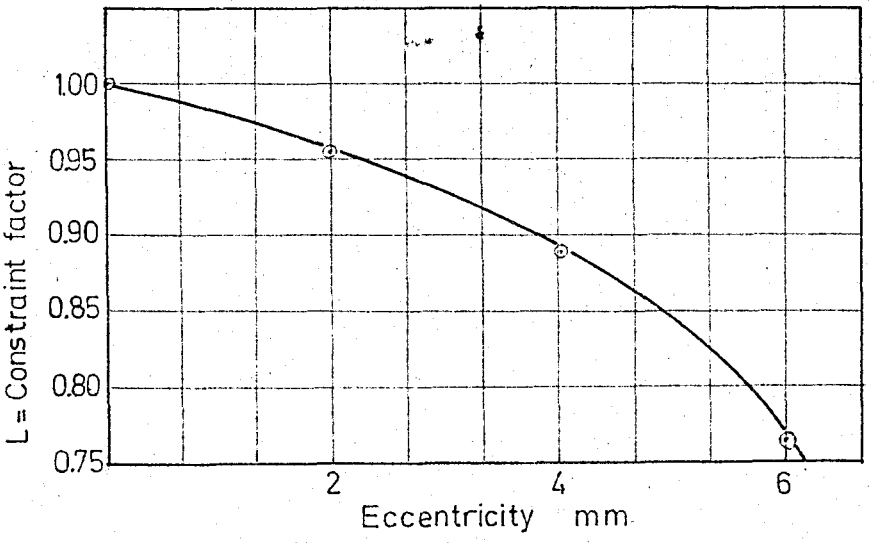

Figure 37

Constraint factor versus eccentricity.

CHAPTER VI

THEORETICAL ANALYSIS

6.1 V-notched Strip Under Tension

The method presented in Chapter II is used to determine the analytical results. If region 2 and 3 of Fig.13 yield first, then from Eq. 2.12 we have

$$\frac{1}{3}\left(a_2^2 + 3b_2^2\right) = k^2$$
$$\frac{1}{3}\left(a_3^2 + 3b_3^2\right) = k^2 \qquad (6.1)$$

Since we know β , Equation (6.1) can be solved for λ , and Mo in terms of P and k after proper substitution is made. The cases considered and results obtained are tabulated in Table 6.

TABLE 6 : Analytic results of V-notched strips.

α = Half notch angle	60°	67°	75°	85°
β	30°	23°	15°	5°
λ	0.51	0.48	0.47	0.43
m° k/P	1.1310	1.1304	1.1266	1.050

We change the results obtained for the lower bound m° into constraint factors as follows.

From Figure 13 , we can write the following relation:

$$L = \frac{q\, m^\circ}{\sigma_o} \qquad (6.2)$$

where L is the constraint factor, q is as defined in Fig. 13 , m° is the lower bound, and σ_o is the yield stress in simple tension.

Also

$$m^\circ p A_T = m^\circ q A \tag{6.3}$$

where A_T is the total cross-section of the specimen, A is the net cross-section between two notch roots, and p is the tensile stress divided by m° at impending plastic flow.

Combining Equations (6.1) and (6.3) and noting that $\sigma_o = \sqrt{3}k$ result into

$$L = \frac{1}{\sqrt{3}} \frac{A_T}{A} \frac{p m^\circ}{k} \tag{6.4}$$

TABLE 7: Summary of lower bound calculations

α	60°	67°	75°	85°	90°
β	30°	23°	15°	5°	0°
$\frac{A_T}{A}$	1.750	1.750	1.750	1.750	1.000
$\frac{p m^\circ}{k}$	1.1310	1.1304	1.1266	1.0500	1.000
L_{LOWER}	1.1434	1.1428	1.1380	1.0600	1.000

Plotting these values, L versus notch angle, the graph in Fig. 30 is obtained. Hill's upper bound which has been superimposed in Fig. 30 was proved by Bishop to be the true solution (28). Values of Hill's upper bound are given in Table 8.

TABLE 8 : Values of Hill's upper bound.

α	70°	75°	80°	85°	90°
L_{UPPER}	1.155	1.141	1.105	1.060	1.000

6.2 Semi-circularly Notched Strip

For the two samples tested with a notch radius of 7.5 mm. an average stress of 40 ksi was obtained as indicated in Table 4 . Here, for the theoretical analysis of the semi-circularly notched specimen, the use of a graph (Fig. 31 drawn by Lianis and Ford (28)) will be made. There the ratio $(a/(a+\rho))$ is plotted versus the constraint factor L, where ρ is the radius of the notch, (a) is the net width between notches.

For this case, $(a/(a+\rho)) = 0.727$. The corresponding point on the graph is 1.108 (Fig. 38). The constraint factor experimentally determined is 1.111.

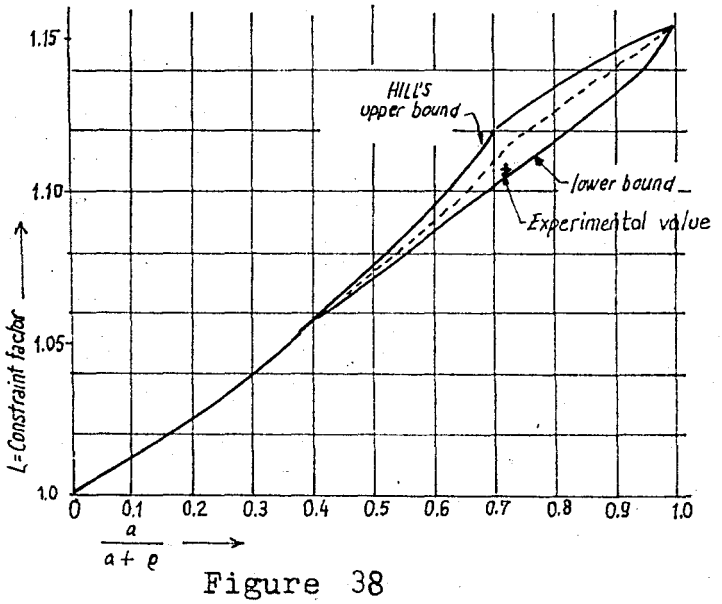

Figure 38
Semi-circularly notched strip under tension

As it is seen from the graph, experime tally determined point is between the theoretical lower bound and the mean value of two bounds.

CHAPTER VII

DISCUSSION OF RESULTS AND CONCLUSION

The results obtained on V-notched strips can be classified as good. Certainly better results could have been obtained if a testing machine of better type, probably a hydraulicly run one was provided. Due to the fact that not all the samples had a uniform composition, as hardness tests proved, results have differed by a few percent for some samples of the same notch angle. No matter what the diversion from the actual values is, one fact became experimentally clear that additional material to specimen without any notches didn't decrease its strength. The increase in the yield load was detected as having a maximum value for $0 \leq \alpha \leq 70$ half notch angle Fig. 30 .

The results obtained experimentally are in good agreement with the analytically obtained results in Table 7. Deviation in all cases is less than 1 %. From Fig.31 it appears that the half angle α where the constraint factor begins to decrease is between 60° - 70° *. For smaller values of α there is a constant lower bound which corresponds to maximum constraint factor 1.15.

Figure 25 shows clearly the regions of high stress concentration. Observations of the samples after they were tested revealed that almost up to 120° , stress concentration effect, though very strongly detected, didn't vary much from one sample to the other. Deformation of the grid lines over the surface of a 150° notched specimen weren't as much as that of a specimen with a 90° notch angle around the root of the notch.

A carefull observation over the polished surfaces of the notched specimens shows that there is a limited zone of penetration

---

* Lianis and Ford (28) showed that α is 67°.

of Leuder's Lines as shown in Fig. 39 . The angles measured between the limiting lines of pentration for each specimen are as follows:

α	ψ
30°	127°
45°	134°
60°	135°
75°	-

ψ is indicated in Fig. 39 . This reveals the fact, that up to $\alpha \cong 70°$ not all of the material around the sides of the notch is plastic. It is the extra elastic material which constraints the plastified portion from flowing continuously. It is important to see that as we have an elastic zone up to $\alpha \cong 70$ we would of course expect to have a rather constant constraint factor. The whole area in the region R , as shown in Fig. 39, is fully plastified. No Leuder's Lines in R are detected around the notch sides. α is 75° .

In the second series of experiments, samples with square cut-outs proved to be the weakest of the series with 34.5 ksi average stress at yield. The effect of the stress concentration was detected to be equally strong for four corners of the square, Fig. 34. Member with parallelogram hole gave a higher yield load then the square. However, two of its corners in the transverse axis were under high stress concentration that first cracks initiated there.

In all cases, the natural iron-oxide coating of the hot-rolled samples acted as a stresscoat. Highly plastified zones were visible due to the flackening out of the brittle coating.

We have observed a very high strains in strips with eccentric holes and lower yield loads. This may be due to premature

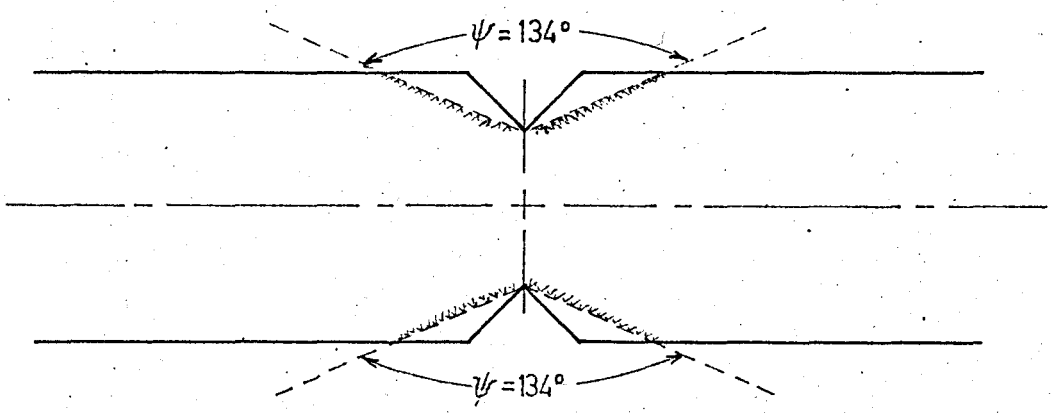

(a) $\alpha = 90^\circ$

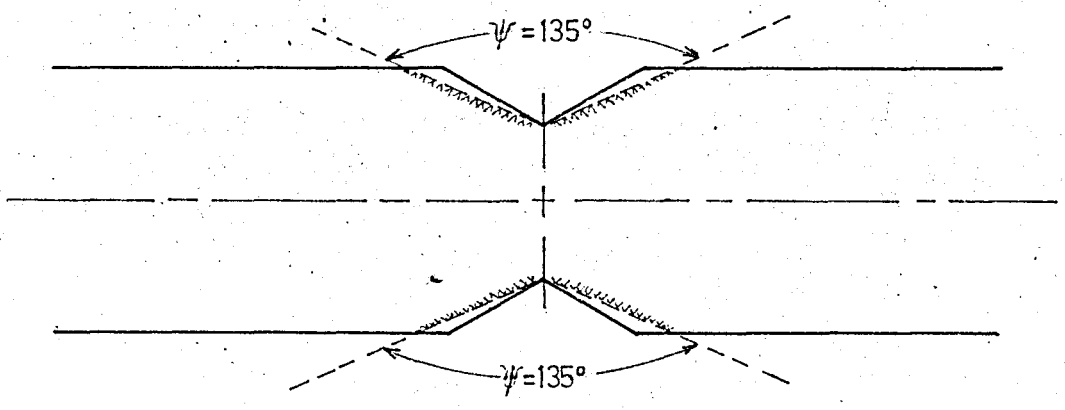

(b) $\alpha = 120^\circ$

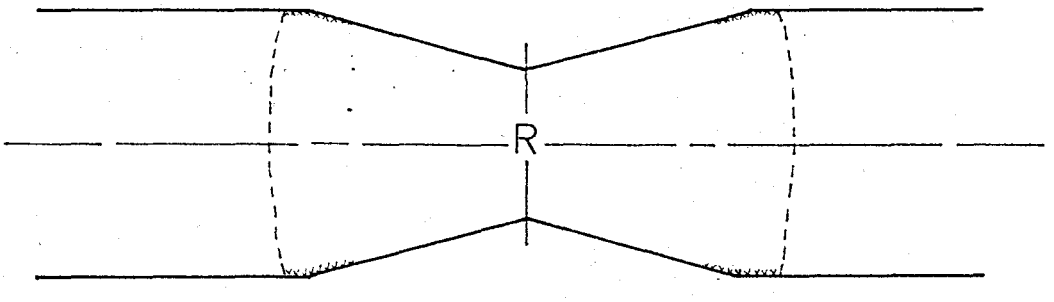

(c) $\alpha = 150^\circ$

Figure 39

Limiting lines of penetration of Leuder's Lines.

plastic yielding in the narrower cross section. Due to the eccentricity, the member will be subjected to a bending moment which will disturb the stress pattern in each of the cross-sections. It could be that for this reason that the manual of AISC-Manual of Steel Construction (29) specifies at least a 15 % reduction in the net cross-section area of a tension member with a hole for sake of safety, or uncertainity of the yield point of the member. The lowest value of the average stress obtained under the yield load is 26500 psi for an eccentricity of 6mm. Then for $\sigma_o = 36000$ psf , the decrease in the yield load is about 25 %. An eccentricity of 4mm resulted in 11.1 % reduction. Therefore it is reasonable to have a reduction of at least 15 % in the net section of the members with holes which are subjected to tension.

For shapes other than notched ones, the strips with a concentrically located holes proved to be the best of the cut-out series.

CHAPTER VIII

REFERENCES

1. Hill, R., The Mathematical Theory of Plasticity, The Oxford Engineering Science Series, Oxford at the Clorendon Press, 1964.

2. Mendelson, A., Plasticity : Theory and Application, The Macmillan Company, New York 1968.

3. Neal, B.G., The Plastic Methods of Structural Analysis, John Wiley & Sons, Inc., New York 1963.

4. Johansen, K.W., Yield-Line Theory, Cement and Concrete Association. William Clowes and Son, Limited, London 1962.

5. Brooks, H., Mason, N.H., Promisel, N.E., Cooper, G.H., Advances in Materials Research in the NATO Nations, The Macmillon Company, New York 1963.

6. Prager, W. and Hodge, P.G. Jr., Theory of Perfectly Plastic Solids, John Wiley and Sons, Inc., New York, Second Printing, 1961.

7. Shanley, F.R., Strength of Materials, Mc Graw-Hill Book Company, Inc., New York 1957.

8. Nadai, A., Plasticity, Engineering Societies Monographs, Mc Graw-Hill Book Company, Inc., New York 1931.

9. Sokolnikoff, I.S., Mathematical Theory of Elasticity, Mc Graw-Hill Book Company, Inc., New York 1956.

10. Dally, J. and Riley, W., Experimental Stress Analysis, Mc Graw-Hill Book Company, New York 1965.

11. Drucker, D.C., A Definition of Stable Inelastic Material, Journ. Appl. Mech. Vol. 26, Transc. ASME,Vol. 81, pp. 101-109, 1959.

12. Greenberg, H.J. and Prager, W., On Limit Design of Beams and Frames Proceedings, Amer. Soc. Civ. Engrs., 77 Separate No. 59, 1951.

13. Moore, M.B., Principles of Stress Analysis, Prentice-Hall, Inc., New York 1954.

14. Hetenyi, M., Handbook of Experimental Stress Analysis, John Wiley and Sons Inc., New York 1950.

15. Juvinall, C.R., Stress, Strain and Strength, Mc Graw-Hill Book Company, New York 1967.

16. Durelli, A.J., Philips, E.A., Tsao, C.H., Introduction to the Theoretical and Experimental Analysis of Stress and Strain, Mc Graw-Hill Book Company, Inc., New York 1958.

17. Hill, R., The Plastic Yielding of Notched Bars under Tension, Quart. Journ. Mech. and Appl. Math., Vol. 2, Pt. 1, pp. 40-52, 1949.

18. Hill, R., On Discontinuous Plastic States, with Special Reference to Localized Necking in Thin Sheets, Journal of Appl. Mech. and Physics of Solids, 1952, Vol. 1, pp. 19-30.

19. Lee, E.H., Plastic Flow in a V-Notched Bar Pulled in Tension, ASME, Journal of Applied Mechanics, Vol. 19, Sept 1952, pp331-6.

20. Hodge, P.G.Jr., Yield Conditions in Plane Plastic Stress, J. Math. Phys. 29, 1950, pp. 38-48.

21. Drucker, D.C., On Obtaining Plane Strain or Plane Stress Conditions in Plasticity, U.S. National Congress of Applied Mechanics Proceeding, ASME, pp. 485-488.

22. Findley, W.N., Drucker, D.C., An Experimental Study of Plane Plastic Straining of Notched Bars, Journal of Applied Mechanics Vol. 32, Sept. 1965 - pp 493-503.

23. Mura, T., Rimawi, W.H., Lee, S.L., Extended Theorems of Limit Analysis, Quarterly of Applied Mathematics, Vol. XXIII, No.2, July 1965, pp. 171-179.

24. Rimawi, W.H., Lee, S.L., Mura, T., Limit Analysis of Notched Tension Specimens, Journal of the Engineering Mechanics Division Proceedings of the American Society for Civil Engineers, Vol.92, No. EM1, Proc. Paper 4636, February 1966, pp. 11-24.

25. Bacha, C.P., Schwalje, J.L., Del Mastro, A., Elements of Engineering Materials, Harper & Brothers Publishers, New York 1957.

26. Van Vlack, L.H., Elements of Material Science, Second Edition, Addison-Wesley Pub. Comp. Inc. Reading. Mass. U.S.A., 1964.

27. Dove, R. C., Paul, H. Adams, Experimental Stress Analysis and Motion Measurements, Charles E. Merill Book Inc., Columbus, Ohio, Second Printing, Copyright 1964.

28. Ford H. and Lianis, G. Plastic Yielding of Notched Strips Under Conditions of Plane Stress, ZAMP, Vol. VIII, 1957. pg. 360-382

29. Manual of Steel Construction, American Institute of Steel Construction, Inc., Sixth Edition, New York, 1965.

30. Lee, G. H., An Introduction to Experimental Stress Analysis, John Wiley and Sons Inc., New York 1956.